GABAergic and Glutamatergic Efferents of the Mouse Ventral Tegmental Area

Research Article

The Journal of Comparative Neurology
Research in Systems Neuroscience
DOI 10.1002/cne.23603

GABAergic and Glutamatergic Efferents of the Mouse Ventral Tegmental Area

Authors: Seth R Taylor[1], Sylvia Badurek[2*], Ralph J DiLeone[1, 5], Raad Nashmi[3], Liliana Minichiello[2, 4], Marina R Picciotto[1, 5]

Institutional Affiliations: [1] Interdepartmental Neuroscience Program, Yale University, New Haven, CT, 06519; [2] European Molecular Biology Laboratory, Monterotondo, Italy; [3] Department of Biology, University of Victoria, Victoria, British Columbia V8P 5C2, Canada; [4] Department of Pharmacology, University of Oxford, OX1 3QT, Oxford, UK;

[5] Departments of Psychiatry and Neurobiology, Yale University, New Haven, CT, 06519

*Current address: Campus Science Support Facilities GmbH, 1030, Vienna, Austria.

Running Head: Mouse VTA Projections

Associate Editor: Paul Sawchenko

Key Words: mesolimbic system, dopamine, lateral habenula, ventral pallidum, retrograde, VGluT2, AB_90755, AB_390204, AB_1091086, AB_1640532, AB_300798, AB_2079751, AB_10807945, AB_10013483, AB_2301998, AB_2311977, nif-0000-30467

Correspondence to Marina R. Picciotto, Department of Psychiatry, Yale University School of Medicine, 34 Park Street, Third Floor Research, New Haven, CT 06508,

USA. Phone: (203) 737-2041. E-mail: marina.picciotto@yale.edu

Grant Support: This work was supported by NIH grant DA14241 from the National Institute on Drug Abuse (M.R.P.), the National Science Foundation (NSF) DGE-1122492 (S.R.T) the State of Connecticut, Department of Mental Health and Addiction Services, and ESTAR fellowship funded by the EC's FP6 Marie Curie host fellowship for Early Stage Research Training (MEST-CT-2004-504640) (S.B.).

Received: Aug 13, 2013; Revised: Apr 02, 2014; Accepted: Apr 03, 2014

Abstract

The role of dopaminergic (DA) projections from the ventral tegmental area (VTA) in appetitive and rewarding behavior has been widely studied, but the VTA also has documented DA-independent functions. Several drugs of abuse, including nicotine, act on VTA GABAergic neurons, and most studies have focused on local inhibitory connections. Relatively little is known about VTA GABA projection neurons and their connections to brain sites outside the VTA. In this study, we employed viral-vector mediated cell-type specific anterograde tracing, classical retrograde tracing and immunohistochemistry to characterize VTA GABA efferents throughout the brain. We found that VTA GABA neurons project widely to forebrain and brainstem targets, including the ventral pallidum, lateral and magnocellular preoptic nuclei, lateral hypothalamus and lateral habenula. Minor projections also go to central amygdala, mediodorsal thalamus, dorsal raphe and deep mesencephalic nuclei, and sparse projections go to prefrontal cortical regions and to nucleus accumbens shell and core. Importantly, these projections differ from the major VTA DA target regions. Retrograde tracing studies confirmed results from the anterograde experiments and differences in projections from VTA subnuclei. Retrogradely-labeled GABA neurons were not numerous and most non-TH/retrogradely labeled cells lacked GABAergic markers. Many non-DA/retrogradely labeled cells projecting to several areas express VGluT2. VTA GABA and glutamate neurons project throughout the brain, most prominently to regions with reciprocal connections to the VTA. These data indicate that VTA GABA and glutamate neurons may have more dopamine-independent functions than previously recognized.

Introduction

The ventral tegmental area (VTA) is involved in motivated, appetitive and reward-related behaviors (Fields et al., 2007). Although the VTA is generally known as the source of dopaminergic (DA) projection neurons, it contains multiple cell types: DA (~60% of VTA cells in the rat), a subset of which express VGluT2 and release glutamate, GABAergic (~35% of cells) and purely glutamatergic neurons (~2-5% of cells, though some reports indicate a higher percentage), which are interspersed, but not equally distributed, among the subregions of the VTA (Yamaguchi et al., 2007; Nair-Roberts et al., 2008; Yamaguchi et al., 2011). VTA DA neurons, including those also expressing VGluT2, project heavily to several limbic structures, including the nucleus accumbens (NAcc), amygdala, and prefrontal cortex (PFC). In the rat, both GABAergic and glutamatergic neurons form local synapses in the VTA (Omelchenko and Sesack, 2009; Dobi et al., 2010) and project in parallel with the DA neurons to limbic regions (Swanson, 1982; Van Bockstaele and Pickel, 1995; Carr and Sesack, 2000a; Yamaguchi et al., 2011). Studies of VTA function have focused largely on the DA projections from the VTA, as these neurons are the most abundant VTA cell type. In addition, drugs abused by humans increase DA levels in VTA projection areas (Di Chiara and Imperato, 1988). However, early anatomical studies also identified substantial non-DA projections from the VTA to several brain regions (Swanson, 1982; Klitenick et al., 1992). These studies combined retrograde tracing with immunohistochemical detection of tyrosine hydroxylase (TH), a dopamine-synthetic enzyme. Retrogradely-labeled neurons that were TH-negative were assumed to be GABAergic, but this has rarely been tested directly (Swanson, 1982; Klitenick et al., 1992; Carr and Sesack, 2000a).

Several lines of evidence indicate that VTA GABA neurons may have important functions independent from local inhibition of VTA DA neurons. Although all drugs abused by

humans increase DA levels in VTA projection target regions, not all of these drugs act directly or exclusively on DA neurons. Many drugs act on inhibitory GABAergic neurons, including alcohol, tetrahydrocannabinol (THC), opiates, benzodiazepines, and nicotine. Descriptions of the mechanisms underlying the addictive properties of these drugs have focused on local GABAergic inhibition of VTA DA neurons (Johnson and North, 1992; Mansvelder and McGehee, 2002; Szabo et al., 2002; Tan et al., 2010; Tolu et al., 2013); however, DA-independent effects of these drugs have also been proposed (Laviolette et al., 2002). Recent studies using transgenic mice to monitor and drive VTA GABA neuron activity have shown that these neurons increase their firing rate in response to cues predicting reward and in response to aversive stimuli (Cohen et al., 2012; Tan et al., 2012). A deeper understanding of the VTA GABAergic system and its projections may therefore be critical for understanding the circuits involved in reward and in the addictive properties of these drugs of abuse.

The connectivity of VTA GABA neurons within the mesocorticolimbic circuitry provides further evidence of roles for VTA GABA neurons beyond local inhibition of VTA DA neurons. Ultrastructural studies have demonstrated striking and distinct specificity of excitatory PFC inputs onto VTA DA and GABA neurons, such that PFC inputs synapse onto GABA neurons projecting to NAcc and not to PFC, but onto DA neurons projecting to PFC and not NAcc (Carr and Sesack, 2000b). A recent study using optogenetic methodology also suggested that VTA GABA neurons selectively innervate cholinergic interneurons in the striatum (Brown et al., 2012).

To date, the majority of published studies on VTA projections have characterized the rat VTA. The ability to identify and manipulate specific cell types using genetically modified mice has increased the use of mice for functional studies of the VTA and connected circuitry.

Knowledge of the mouse VTA and its projections has focused on dopaminergic circuits (Lammel et al., 2008; Lammel et al., 2011), but is not as well characterized as the rat. In addition, recent reports have described both DA/VGluT2 neurons and non-DA, VGluT2-expressing neurons in the rodent VTA (Kawano et al., 2006; Yamaguchi et al., 2007; Hnasko et al., 2012). Some of these putative glutamatergic neurons project from the VTA to PFC, NAcc, and other limbic structures (Yamaguchi et al., 2011; Gorelova et al., 2012; Hnasko et al., 2012), thus raising the possibility of more widespread VTA glutamatergic projections. Therefore, in this study we employed viral-vector mediated cell-specific anterograde tracing in combination with classical retrograde tracing in transgenic mice allowing for improved detection of GABAergic and glutamatergic neurons to provide more in depth characterization of non-dopaminergic projections from the mouse VTA.

Materials and Methods

Animals

All animal studies were carried out in accordance with the standards and procedures for animal care and use established by the National Institutes of Health and were approved by the Yale University Animal Care and Use Committee. Three lines of transgenic mice targeting GABA neurons via glutamic acid decarboxylase (GAD) promoters were used in this study: GAD67-Cre (Ohtsuka et al., 2013), GAD65-IRES-Cre (Jackson Labs, Stock #010802) and GAD67-GFP knock-in mice (Tamamaki et al., 2003). In addition, VGluT2-IRES-Cre mice (Jackson Labs, Stock #016963) were used to identify VTA neurons expressing the vesicular glutamate transporter (VGluT2). In the transgenic lines, both males and females were used because no differences were observed between genders. The lines had been backcrossed onto

C57BL/6J mice for: GAD67-Cre, 4 generations; GAD65-IRES-Cre, 2-4 generations; GAD67-GFP, 10 generations; VGluT2-IRES-Cre, 6 generations.

Anterograde Tracing

GAD67-Cre and GAD65-IRES-Cre mice (12-16 weeks old) received VTA infusions of adeno-associated viruses (AAVs) driving Cre-dependent channelrhodopsin-fluorescent protein fusions (eYFP or mCherry; UNC Vector Core) by pressure injection in a stereotaxic frame (Kopf Instruments, Tujunga, CA) under isoflurane anesthesia (VetEquip, Pleasanton, CA). Table 1 describes the viruses used including their sources. Coordinates for VTA infusions were, from bregma, AP: -2.9 to -3.1 mm; ML: +0.35 mm; DV: -4.65 mm. 0.2 – 0.5 µl of virus was infused unilaterally by pressure injection through pulled glass micropipettes with tips of 10-20 µm inner diameter. Animals were kept warm until they had awakened and were returned to their home cages. Survival times ranged from 21-28 days to ensure robust expression and trafficking of fluorescent proteins to distant terminals.

Retrograde Tracing

For retrograde experiments, 50-100 nl of FluoroGold (FG, Fluorochrome, Inc., Englewood, Co; 1% in phosphate-buffered saline; PBS) or Red Retrobeads IX (beads, LumaFluor, Inc.) was infused by pressure injection through glass micropipettes (tips of 10-20 µm inner diameter for FG, 50-60 µm inner diameter for beads) into several brain regions of GAD67-GFP knock-in mice (8-12 weeks old). Coordinates for retrograde infusions were (all from bregma): NAcc shell (n=4); AP +1.8 – 2.0 mm, ML 0.55-0.6 mm, DV -4.75 mm; NAcc Core (n=3); AP +1.5 mm, ML +1.35 mm, DV -4.7 mm; lateral habenula (LHb; n=3): AP -1.9

mm, ML 0.6 mm, DV -3.2 mm; Amygdala (n=3): AP -1.9 mm; ML 3.25 mm, DV -4.9 mm; ventral pallidum (VP; n=3): AP +0.7 mm, 0.55 mm, -5.0 mm; magnocellular preoptic nucleus (MCPO; n=2): AP +0.45 mm, ML 1.2 mm, DV -5.6 mm. All infusions were unilateral. Following surgery, animals were returned to home cages to allow for transport of the tracer. The survival time was seven days for FG and 21 days for beads.

For retrograde labeling of VGluT2+ neurons, VGluT2-IRES-Cre mice (8-10 weeks old, n=2 for each target region) received two intracranial infusions. First mice received infusions of FG, as above, into one of the seven target regions, and subsequently all mice received infusions of AAV-DIO-Ef1a-mCherry into the VTA (coordinates the same as for anterograde tracers above). Survival time was 14 days.

Tissue processing and Immunohistochemistry

For all tracing experiments, animals were injected with an overdose of chloral hydrate (15% in PBS) and transcardially perfused with ice-cold PBS (pH 7.4) followed by ice-cold 4% paraformaldehyde (PFA) in PBS (pH 7.4). Brains were removed and post-fixed overnight in 4% PFA, then cryoprotected in 30% sucrose in PBS at 4º C until they sank. For anterograde tracing, brains were sectioned from the rostral pole of cortex through the cerebellum in six series of 40 µm thick sections on a sliding microtome (Leica Biosystems, Buffalo Grove, IL), resulting in series with sections 240 µm apart. One entire series was stained, imaged and analyzed to determine anterograde projections. For retrograde tracing, six series of 50 µm thick sections were taken through the injection site and 25 µm thick sections were cut through the VTA for analysis. All of the sections containing VTA from a single series (5-6 sections) were stained and imaged to count retrogradely labeled cells.

For immunohistochemical staining, free floating sections were washed 3 x 5 minutes in PBS at room temperature, then blocked for 1 hour in 10% Normal Donkey Serum (Jackson ImmunoResearch) with 0.3% Triton X-100 in PBS. Sections were then transferred to primary antibody solutions (all antibodies diluted in PBS with 0.3% Triton X-100) and incubated overnight at 4º C (see Table 2 for sources and dilutions of primary antibodies). In cases of double and triple labeling, sections were incubated in solutions containing multiple primary antibodies raised in different host species. Sections stained for GAD67 were incubated in primary antibody at 4º C for three nights without Triton X-100, then any additional antibodies for double or triple labeling were added on the third day for overnight incubation. After three 5 minute washes in PBS at room temperature, sections were incubated in the appropriate combinations of secondary antibodies (AlexaFluor 405 Donkey anti-Sheep IgG, 1:500; DyLight 488 Donkey Anti-Chicken IgY, 1:1000; AlexaFluor 555 Donkey anti-Rabbit, 1:1000; AlexaFluor 647 Donkey Anti-Goat, 1:500) for two hours at room temperature. Sections were washed 3 times for 5 minutes in PBS, mounted on SuperFrost Plus Slides (Fisher Scientific) and coverslipped with FluoroMount G (Electron Microscopy Sciences, Hatfield, PA). Incubations were carried out in light-protected conditions to preserve endogenous fluorescence of the tracers and virally-infected cells. Secondary antibodies were obtained from Invitrogen or Jackson ImmunoResearch.

Antibody Characterization

Sheep anti-tyrosine hydroxylase, polyclonal

According to the manufacturer (Millipore, Billerica MA; Cat. No. AB1542, RRID: AB_90755), the primary antibody was raised against native tyrosine hydroxylase (TH) from rat

pheochromocytoma cells. Western blot analysis revealed on mouse brain lysate revealed one band of ~60 kDa. The staining we observed in the ventral midbrain matches published reports of TH staining in the VTA and substantia nigra (Swanson, 1982).

Rabbit anti-tyrosine hydroxylase, polyclonal

According to the manufacturer (Millipore, Cat. No. AB152, RRID: AB_390204), the primary antibody was raised against denatured TH from rat pheochromocytoma cells (denatured by sodium dodecyl sulfate). The manufacturer's specification sheet indicates that western blot analysis labels a single band ~60-62 kDa. The staining pattern we observed was restricted to cells with the classical dopaminergic localization in mouse brain (Swanson, 1982).

Chicken anti-tyrosine hydroxylase, polyclonal

According to the manufacturer (Thermo Scientific Pierce Antibodies, Cat. No. PA1-46351; RRID: AB_1091086), the primary antibody was raised against two separate peptide sequences, one from between amino acids 1-100 of the N terminus of mouse tyrosine 3-monooxygenase, and the second peptide from between amino acids 398-498 of the C-terminus of the same protein. The staining pattern we observed was identical to staining with other anti-tyrosine hydroxylase antisera.

Goat anti-glutamate decarboxylase 67 polyclonal

According to the manufacturer (Abcam, Cambridge, MA; Cat. No. ab80589; RRID: AB_1640532), the primary antibody was raised against a synthetic peptide: C-PDSPQRREKLHK, which corresponds to internal sequence amino acids 526-537 of human GAD67. The manufacturer states that the antibody reacts with human, mouse and rat GAD67 with no expected cross-reactivity with GAD65. Western blot analysis of mouse brain lysate performed by the manufacturer selectively labels a single band at 67 kDa.

Chicken anti-green fluorescent protein polyclonal

According to the manufacturer (Abcam, Cat. No. ab13970, RRID: AB_300798), this primary antibody was raised against recombinant full length GFP and recognizes enhanced GFP as well as all the fluorescent proteins by the jellyfish *Aequorea victoria*, including yellow fluorescent protein (YFP). The manufacturer's specification sheet indicates that western blot analysis of transgenic mouse spinal cord selectively labels a band at ~27 kDa. In our hands, this antibody does not stain wild-type brain tissue which lacks GFP or YFP.

Goat anti-choline acetyltransferase (ChAT) polyclonal

According to the manufacturer (Millipore, Cat. No. AB144P, RRID: AB_2079751), the primary antibody was raised against human placental ChAT. Western blot analysis of mouse brain lysate reveals one band at 70 kDa (manufacturer's information). In our experiments, staining was visible in cell bodies, dendrites and axons and was restricted to previously documented cholinergic regions (Ruggiero et al, 1990).

Rabbit anti-NeuN polyclonal

This antibody (Millipore, Cat. No. ABN78, RRID: AB_10807945) was raised against a GST-tagged recombinant protein corresponding to mouse NeuN, and recognizes bands at 46 and 48 kDa in western blot analysis of mouse brain nuclear extract (manufacturer's information). The antibody strongly labeled nuclei throughout the brain in our hands.

Rabbit anti-dsRed polyclonal

This antibody (Clontech, Mountain View, CA; Cat. No. 632496, RRID: AB_10013483) was raised against DsRed-Express, a variant of red fluorescent protein from *Discosoma* species, and recognizes DsRed and variants, including mCherry, and N- and C-terminal fusion proteins with these DsRed variants. Western blot analysis of HEK293 cells stably expressing DsRed showed a

specific band of 30-38 kDa (manufacturer's information). In our hands, no staining was seen in animals lacking mCherry expression.

Rabbit anti-vesicular GABA transporter (VGAT) polyclonal

This antibody (Millipore, Cat. No. AB5062P, RRID: AB_2301998) was raised against a 17 amino acid synthetic peptide corresponding to the last 17 amino acids at the carboxy terminal of rat VGAT (VHSLEGLIEAYRTNAED). This antibody detected only one band of ~51 kDa in western blot analysis of mouse brain lysate (Wang and Sun, 2012). The pattern of staining in our hands was similar to published reports (Wang and Sun, 2012).

Rabbit anti-FluoroGold polyclonal

This antibody (Fluorochrome, Inc., Denver CO, RRID: AB_2311977) was raised in rabbit against FluoroGold (hydroxystilbamidine) and did not stain tissue negative for FluoroGold in our hands.

Imaging/Counting

Sections from virally-infused brains for anterograde tracing were imaged on an epifluorescent Zeiss Axio Scope. Mosaics of the hemisphere ipsilateral to the infusion site were taken with a 10x objective and excitation and emission filters for Alexa Fluor 488, 555 and 647 signals. Images were analyzed for presence of fluorescent fibers throughout the brain offline using Adobe Photoshop CS6.

Sections from brains infused with retrograde tracers were imaged on an Olympus FV1000 laser-scanning confocal microscope equipped with the following lasers: 405 nm diode, 488 Argon, 543 HeNe, and 633 HeNe. VTA sections containing retrogradely labeled cells were identified under epifluorescence using excitation and emission filters for rhodamine and then

consecutive series of images with AF 405, 488, and 546 channels were taken with a 20x oil immersion objective (NA 0.85) at 1.64 µm steps along the z-axis, resulting in 10-12 optical sections. Higher magnification images of individual neurons were taken with a 60x oil immersion objective (NA 1.42) or 100x objective (NA 1.40). Consecutive images of VGAT stained tissue were taken with the 60x objective and a 2x or 2.5x digital zoom at 0.4 µm steps along the z-axis.

For quantification of retrogradely labeled cells, two non-overlapping z-stacks were acquired to cover the entire medial to lateral extent of the VTA ipsilateral to tracer injection. Retrogradely labeled cells were counted from one single optical section from each z-stack. Optical sections for counting were selected randomly from each z-stack, but only if clearly defined cell bodies were visible in all the acquired channels. Sections containing the tissue surface were avoided. Optical sections at the same focal plane were selected from the medial and lateral stacks of the same physical section. Cells were counted using Adobe Photoshop CS6. The morphology and arrangement of DA neurons were used to identify the subnuclei of the VTA following published atlases (Paxinos et al., 2001). The number of TH+, GFP+ (or GAD67+ for some sections), and retrogradely labeled cells (FG+ or beads+) was counted and marked in individual channels. Then by combining the TH/retrograde or GFP/retrograde channels, the number of TH/retrograde, GFP/retrograde and TH(-)/ GFP(-)/retrograde cells was counted within each of the subnuclei of the VTA. For each animal, the number of TH+, GFP+, retrogradely labeled, TH+/retrogradely labeled, GFP+/retrogradely labeled, and non-TH/non-GFP/retrogradely labeled cells was totaled within each subnucleus (rostral linear nucleus (RLi), interfascicular nucleus (IF), parabrachial pigmented nucleus (PBP), paranigral nucleus (PN), caudal linear nucleus, CLi). For VGluT2-IRES-Cre animals, cells were counted in the same

fashion, and the number of TH+, VGluT2+ (as marked by mCherry expression), and FG+ cells were counted and marked. By combining the channels, the numbers of TH+/FG+, TH+/mCherry+/FG+, mCherry/FG+, and FG+ only labeled cells were counted and totaled within the VTA subnuclei. These totals were averaged across all the animals for each infusion region, and the percentages of retrogradely labeled cells that were also positive for TH or GFP (for GAD67-GFP mice), and for TH or mCherry (for VGluT2-IRES-Cre mice) or negative for both markers were calculated.

Images taken to identify YFP+/VGAT+ terminals were analyzed in Olympus FV10-ASW 3.0 Viewer software. All figures were prepared using Image J (NIH, rsb.info.nih.gov/ij/index.html, RRID: nif-0000-30467) and Adobe Photoshop CS6 software. For some images, brightness and contrast were adjusted, but no other manipulations were made.

Results

Viral injection of Cre-reporter constructs detects GABAergic cells in the VTA of GAD65-IRES-Cre and GAD67-Cre mice

AAV-Ef1a-DIO-mCherry was infused into the VTA and used as a marker in Cre recombinase-expressing mice to identify GABAergic neurons. Infusion of AAV-Ef1a-DIO-mCherry into the VTA of both GAD65-IRES-Cre and GAD67-Cre mice revealed mCherry expression in GABAergic neurons of the VTA (Fig 1A-H). mCherry+ cells stained for GAD67, a GABA-synthetic enzyme, and lacked immunoreactivity for TH (Fig 1C, G, I), indicating a GABAergic, non-DA phenotype. Qualitatively, GAD65-IRES-Cre mice appeared to have more mCherry labeling than did GAD67-Cre mice. In both lines, some mCherry labeled cells did not show distinct GAD67 immunostaining, but were at the same level as the surrounding neuropil.

These cells may still be GABAergic, as immunohistochemical detection of GAD67 cell bodies in the VTA is difficult and underestimates the total GABAergic population (Olson and Nestler, 2007; Nair-Roberts et al., 2008), and these cells were negative for TH (Fig 1D, H, I). GABAergic Cre-expressing cells were present in all subregions of the VTA (RLi, IF, PBP, PN, CLi).

Anterograde Tracing

Twenty-five mice (15 GAD67-Cre, 10 GAD65-IRES-Cre) received infusions of adeno-associated viruses (AAVs) driving Cre-dependent expression of fluorescent proteins into the VTA or surrounding areas. Multiple viruses were used for cell-type specific tracing in order to avoid any virus-specific artifacts (viruses are described in Table 1). All Cre-dependent marker viruses resulted in similar patterns of tracing and fluorescent protein expression. Seven mice (four GAD65-IRES-Cre, three GAD67-Cre,) had infusions almost entirely limited to the VTA, and three GAD67-Cre mice had control infusions in surrounding areas that spared the VTA. These ten mice were chosen for further analysis. Injection of AAV-Ef1a-DIO-ChR2-eYFP, AAV-Ef1a-DIO-SynB2-GFP, or AAV-Ef1a-DIO-ChR2-mCherry led to cell body labeling throughout the subnuclei of the VTA (Fig 1J, case S2). Labeled cell bodies were found in the IF, RLi, CLi, PBP, and PN nuclei. Figure 2 contains diagrams of the ventral midbrain demonstrating virally-labeled cell bodies from five mice (two GAD65-IRES-Cre, three GAD67-Cre), focusing on those with virus confined mainly within the VTA and those with control infusions excluding the VTA (Cases GC 152, GC 116).

Viral expression restricted to VTA GABA neurons resulted in fluorescent labeling of fibers throughout much of the rostral-caudal extent of the brain. The labeling patterns were

similar across all animals injected, with some slight differences attributable to viral spread. Cases S2, S3 (GAD65-IRES-Cre) and GC153 (GAD67-Cre) had infusions restricted almost entirely to the VTA and are described as representative cases of their respective lines. Cases S2 and GC153 had a few labeled neurons in the interpeduncular nucleus (IPN), while S3 had a small number of labeled neurons in the medial posterior hypothalamus, periaqueductal grey and superior colliculus along the pipette track.

In all animals, ascending fibers were concentrated along the medial forebrain bundle in the ventral portion of the forebrain. The majority of fibers were ipsilateral to the infusion of virus, though in some cases contralateral projections were observed. This may have been due to spread of the virus into both sides of the VTA, since labeled cell bodies were occasionally found bilaterally. Images of several forebrain sections from case S2 are shown in Figure 3. Labeled fibers were thin, often branched, and had bulging varicosities that are commonly accepted to be synaptic contacts (Figure 3D, inset). In contrast to our hypothesis based on published work, only sparse labeling of PFC areas was visible (Fig 3A-C). In some animals, few, if any, fibers were visible in medial pregenual cortical areas (data not shown). The majority of labeled fibers in these cortical regions were concentrated in the deeper layers of cortex. Similarly, innervation of the NAcc core and shell was also sparse (Fig 3D-F). The fibers in NAcc core often were found near the medial portion of the core just below the tip of the ventricle. Fibers in NAcc medial shell were spread throughout the structure. The very few fibers visible in dorsal striatum were located along the lateral ventricle. The major island of Calleja, located between NAcc medial shell and the lateral septum, contained labeled fibers in every animal with VTA injection (Fig 3D-F; Fig 4A-B).

Dense fiber labeling was found in the VP and the lateral preoptic area (LPO) (Fig 3C-I). VTA efferent fibers were present throughout the rostral-caudal extent of the VP, but were more concentrated in the rostral regions. In coronal sections, the rostral pallidum appears as patches separating the NAcc shell and olfactory tubercle. These patches show markedly less TH immunoreactivity than the surrounding ventral striatal regions, but often contained labeled fibers (Fig 4A-B). Further caudal, fibers coursed continuously across the border of the dorsomedial pallidum and the LPO (Fig 3G-I). Figure 4 shows line drawings of sections from a GAD65-IRES-Cre animal (Case S3) and a GAD67-Cre animal (GC 153). The projections of VTA neurons in the two lines displayed only slight differences. At the level of VP, GAD67-Cre animals showed dense labeling in the ventral and lateral portions of pallidum, whereas in GAD65-IRES-Cre animals labeling was restricted to dorsomedial pallidum (Fig 4C-D).

Moderate labeling was seen in several divisions of the bed nucleus of stria terminalis (BNST), including the medial ventral portion just beneath the anterior commissure (Fig 3J-L) and the lateral division, posterior part medial to the internal capsule (Fig 4E-F). The caudal portion of the LPO also showed a dense population of VTA GABA fibers (Fig 3J-L). Case S2 showed labeling in the interstitial nucleus of the posterior limb of the anterior commissure (IPAC) (Fig. 3J-L). GAD67-Cre animals had very little labeling in IPAC nuclei.

GAD67-Cre mice showed extensive VTA GABAergic projections to the MCPO (Fig 4F). Sections from GAD65-IRES-Cre mice had strong labeling in the dorsal portion of the LPO, with some fibers also visible in the BNST divisions, just ventral to the anterior commissure. Only a few fibers were visible in the horizontal limb of the diagonal band of Broca (HDB) and MCPO (Fig 3J-L; 4E-F). These areas are sparsely innervated by dopaminergic fibers (Fig 3J-L).

VTA GABA neurons projected to the LHb in both lines. GAD67-Cre fibers innervated the lateral ventrolateral portion of the LHb, whereas GAD65-IRES-Cre fibers consistently innervated the medial portion (Fig 4G-H; Fig 5A-C). Very few TH+ fibers were present in LHb. In some cases, labeled fibers were seen in the mediodorsal thalamic nucleus. VTA GABA fibers were also visible in the lateral hypothalamus and the amygdala. Among amygdalar nuclei in both GAD65-IRES-Cre and GAD67-Cre mice, labeled fibers preferentially innervated the central amygdala (Fig 4G-H; Fig 5D-F).

Labeled fibers were very concentrated at the injection sites in the VTA (Fig 4K-L). No overlap was seen between labeled cells and TH immunoreactivity. In many cases, the medial terminal nucleus of the accessory optic tract (MT), which borders the lateral portion of the VTA, was heavily labeled. In these cases, fibers were seen in the nucleus of the optic tract (OT) in the dorsal midbrain. Fibers were seen throughout the subnuclei of the VTA and reaching into the neighboring substantia nigra compacta and interpeduncular nucleus (IPN). In some cases, GABAergic neuronal cell bodies of the IPN were clearly labeled by the virus. YFP-labeled fibers in the IPN, therefore, could be from VTA or IPN GABA neurons. The majority of labeled fibers in the IPN were distinct in appearance from fibers in the VTA or forebrain regions; they were dense mesh-like fibers surrounding labeled cell bodies, indicating that they may arise from IPN interneurons, rather than projection neurons. It is still possible that the IPN could receive VTA GABA projections, as the IPN does contain TH+ fibers (data not shown).

In several cases, the ability to identify descending VTA GABAergic projections was complicated by labeling of cell bodies in the IPN, which projects heavily to brainstem nuclei. Nevertheless, some areas of the dorsal midbrain and brainstem displayed consistent labeling across animals, regardless of the extent of IPN labeling (Fig 4M-N). In some cases, cell bodies

were labeled in the A8 dopaminergic nucleus, the retrorubral field (RRF). In most cases, even with no cell bodies visible, fibers were visible in RRF, but these were characteristic of fibers of passage coursing dorsally. Moderate anterograde labeling was seen in the ventral and lateral portions of the periaqueductal gray (PAG, Fig 4M-P). Case S2 showed modest labeling in the median raphe (MnR), including the paramedian portion. Case GC153, which had few labeled cell bodies in IPN, also had labeled fibers in MnR, suggesting a minor VTA GABA projection.

The dorsal raphe contained labeled fibers, particularly in the dorsal, ventral and lateral parts, and in the raphe cap (Fig 4M-P; Fig 5J-L). Some of the fibers in lateral dorsal raphe originated from GABA neurons in lateral PBP, RRF and CLi. Anterograde labeling was visible in the pedunculopontine tegmental nucleus (PPTg), but most of the labeling was characteristic of fibers of passage. All of the analyzed GAD65-IRES-Cre animals showed sparse, but consistent, labeling of the ipsilateral external cortex of the interior commissure (ECIC). GAD67-Cre mice showed labeling in the superior colliculus, both in the superficial and intermediate gray layers. In both GAD67 and GAD65-IRES-Cre lines, the laterodorsal tegmental nucleus (LDTg) contained labeled fibers (Fig 4O-P; Fig 5J-L). Sparse labeling was also seen in the locus coeruleus (LC) in both lines. A few fibers were observed in the ipsilateral lateral and medial parabrachial nuclei (LPBC, MPB). In the ventral brainstem, labeling was seen in the rostral periolivary region (RPO) in some animals. This could have resulted from labeled cells in the red nucleus, as a control infusion (GC 152) centered in red nucleus that spared VTA resulted in heavy projections to RPO and surrounding areas (data not shown).

Table 3 shows the relative density of projections throughout the brain for several cases with virus mainly restricted to the VTA. The results were largely consistent between cases, though some additional differences between GAD65-IRES-Cre and GAD67-Cre mice were

noted. For example, GAD67-Cre mice showed light to moderate labeling in areas lateral to the NAcc (piriform cortex, claustrum, endopiriform nucleus) while GAD65-IRES-Cre mice did not.

Analysis of control infusions of AAV-DIO-Ef1a-ChR2-eYFP (GC 116) or AAV-DIO-Ef1a-ChR2-mCherry (Cases GC 152 and 156) into regions neighboring the VTA revealed patterns of labeled fibers distinct from VTA injections. Case 116 was centered in the IPN, Case 152 was centered in the red nucleus, dorsal to the VTA, and Case 156 was centered in the rostral periaqueductal grey and posterior hypothalamus anterior to the VTA. In contrast to VTA injections, very few, if any, labeled fibers were visible in VP, NAcc, MCPO, LHb, or dorsal raphe. Cases 152 and 156 resulted in extensive labeling in the thalamus and dorsal midbrain, and Case 116 resulted in labeled fibers throughout the median raphe and anterior tegmental nucleus (data not shown).

Brown et al (2012) recently reported that VTA GABA neurons projecting to the NAcc shell selectively target cholinergic interneurons. To identify possible postsynaptic target cells of VTA GABA neurons, we stained for choline acetyltransferase (ChAT), a marker of cholinergic cells, as well as NeuN to visualize all the neurons. We observed labeled fibers that encapsulated ChAT+ cell bodies (Fig 6A-C) in both the NAcc shell and core. These fibers had several varicosities that apposed the soma and dendrites of the ChAT+ neurons. Triple labeling for YFP, ChAT and NeuN showed that labeled fibers also surrounded ChAT-negative cells (Fig 6C).

To verify that YFP+ labeled fibers showed evidence of inhibitory neurotransmission, we performed double staining for YFP and the vesicular GABA transporter (VGAT), the protein that packages GABA into synaptic vesicles at inhibitory terminals. A subset of YFP+ varicosities showed clear co-labeling with VGAT in the LHb (Fig 6D), NAcc shell, major island of Calleja, VP, amygdala, and VTA. This demonstrates that VTA GABA neuron fibers in the areas

mentioned above contain GABAergic varicosities, suggesting the presence of synaptic connections.

Retrograde Tracing

Retrograde labeling experiments were performed in a subset of projection target regions to confirm the specificity of anterograde labeling and to characterize the localization of GABA projection neurons within the VTA. Retrograde tracers (Red Retrobeads IX or Fluorogold) were infused into the NAcc shell, NAcc core, PFC, amygdala, LHb, VP and MCPO of GAD67-GFP knock-in mice and VGluT2-IRES-Cre mice. Injections into VP in most cases included adjacent regions of the bed nucleus of the stria terminalis (BNST) and injections into MCPO often spread into the olfactory tubercle (OT), and are abbreviated as VP/BNST and MCPO/OT, respectively. GAD67-GFP mice were used to facilitate identification of GABAergic neurons within the VTA after pilot immunohistochemistry experiments marked only a small subset of GABAergic cell bodies within the VTA, as others have reported (Fig 7A-D; Olson and Nestler, 2007), and VGluT2-IRES-Cre mice were used to identify glutamate neurons. In some cases, Fluorogold (FG) occasionally diffused more widely from the infusion site than the Retrobeads. FG injections into MCPO/OT and VP/BNST resulted in many more retrogradely labeled neurons in the VTA than did the beads; however, the percentages of TH, GFP, VGluT2 or non-labeled cells were similar across tracers, so the data were analyzed and combined across experiments (Fig 7J-K).

Figure 8 shows representative infusion sites from the seven tested regions. Retrograde infusions in NAcc shell, NAcc core, LHb, amygdala, VP/BNST and MCPO/OT resulted in labeled cells throughout the VTA (Fig 7E-H). Double immunohistochemical staining for GFP

and TH revealed that projections to various target regions differ in neurotransmitter content and in location of origin within the VTA. As no co-localization of GFP and TH was observed in any experiment, retrogradely labeled cells in GAD67-GFP mice were classified as TH+, GFP+, or TH(-)/GFP(-) (Fig 7E-I). The locations of retrogradely-labeled/GFP neurons from a representative case for each infusion site are graphed in Figure 9.

Overall, the majority of GABAergic projections labeled by retrograde tracing originated from the PBP and paranigral PN subnuclei. The RLi and IF had few detectable GABAergic projection cells by retrograde tracing, but had numerous TH(-)/GFP(-)/retrogradely labeled cells. Among the projection target regions, the projection to LHb had the highest GABAergic component, followed by PFC, VP, and amygdala. NAcc core infusions resulted in very few GABAergic retrogradely labeled cells. Unexpectedly, the majority of TH(-)/retrogradely-labeled cells were also GFP(-), especially in the RLi and IF, and in the projection to the LHb. The percentages of retrogradely labeled cells by neurotransmitter phenotype are graphed for each VTA subnucleus and tracer infusion site in the left hand column of Figure 10.

To identify the neurochemical identity of non-dopaminergic, non-GFP/retrogradely labeled cells, we performed another set of retrograde tracing studies in VGluT2-IRES-Cre mice. These mice received two infusions: FG into a target region and AAV-DIO-Ef1a-mCherry into the VTA to visualize VGluT2+ cells. VGluT2+ cells were found throughout the VTA, but were concentrated in the medial nuclei (RLi, IF, CLi), and the medial portions of PBP and PN. There was substantial overlap of VGluT2 with TH. 51% of the VTA TH+ neurons co-expressed VGluT2 (55% in RLi, 67% in IF, 30% in PBP, 66% in PN, 39% in CLi), though our methods were not designed to quantify and estimate the total TH/VGluT2 population rigorously.

Conversely, only 33% of VGluT2+ cells expressed TH (7% in RLi, 18% in IF, 32% in PBP, 54% in PN, and 56% in CLi).

Immunohistochemical detection of TH and FG, along with mCherry expression (VGluT2+), revealed the following classes of retrogradely labeled cells: FG/TH only, FG/TH/VGluT2, FG/VGluT2 only (glutamatergic), and FG/TH(-)/VGluT2(-) (putative GABAergic). Examples of neurons in these classes are demonstrated in Figure 11. The percentages of retrogradely labeled cells by neurotransmitter phenotype are graphed according to VTA subnucleus and tracer infusion site in the right hand column of Figure 10. Table 4 contains the percentages of FG+ cells in each of the four classes by VTA subnucleus and infusion region. These experiments revealed that the vast majority of DA neurons projecting to the amygdala from all regions of the VTA also express VGluT2. The majority of the DA projection neurons in the PN also express VGluT2. This was true for all the target regions tested. In addition to a substantial portion of TH+ projection neurons that express VGluT2, the VTA contains VGluT2 only neurons that project to each area examined. FG/VGluT2 cells were concentrated in the medial aspects of the VTA, and comprised the vast majority of the projections of RLi and IF to VP/BNST and MCPO/OT in particular.

Comparison of the retrogradely labeled cells between experiments in GAD67-GFP and VGluT2-IRES-Cre mice revealed strikingly similar results for the PBP, PN, and CLi subnuclei of the VTA. Retrogradely labeled cells in the RLi and IF subnuclei showed more variability between the two mouse lines, but the differences were primarily in animals with few retrogradely labeled cells in these areas. These data indicate that a substantial proportion of the non-dopaminergic projections from the VTA express VGluT2 and are likely glutamatergic.

Figure 12 shows the locations of FG/VGluT2-only cells from a representative case from each tracer infusion site. These cells were concentrated in the dorsal and medial aspects of the VTA, and were occasionally found in the lateral and ventral regions. In the mouse VTA, these medial areas have fewer dopaminergic cells than the more lateral aspects. This is in contrast to the distribution of VTA GABA projection neurons, which were primarily located in the ventral and lateral aspects of the VTA. In most of the retrograde tracing experiments, a small percentage of the total VTA cells were labeled with tracer. Table 5 shows the percentage of the counted VTA cells of each neurotransmitter phenotype that were retrogradely labeled.

Discussion

In this study we demonstrate that GABAergic and glutamatergic neurons in the mouse VTA project widely to sites throughout the forebrain and brainstem. VTA GABA neurons project primarily to limbic structures other than PFC and NAcc, including the LPO, MCPO, BNST, central amygdala, LHb, and VP, and dorsal raphe. These projection neurons originate from all VTA subnuclei, but are concentrated in the lateral VTA. In addition, retrograde tracing data indicate that the mouse VTA also contains substantial populations of both TH/VGluT2 and VGluT2-only projection neurons. Many of the TH neurons, especially in medial VTA, express VGluT2. TH/VGluT2 neurons project to several forebrain regions, and make up the majority of dopaminergic projections from the paranigral nucleus. VGluT2-only projection neurons are concentrated in the dorsal and medial regions of the VTA and project heavily to LHb, VP/BNST, and MCPO/OT. This indicates that the glutamatergic output of the mouse VTA may be more extensive than previously appreciated. Some of these structures receive only minimal

dopaminergic innervation, indicating that VTA GABA and glutamate projections form circuits distinct from those of neighboring DA neurons.

Technical Considerations

A number of methodological issues should be considered as potential caveats for the current study. Tracer uptake by damaged fibers of passage could result in false positive labeling, but we feel this does not confound our results for several reasons. Virally-labeled cell bodies were restricted to injection sites, indicating that viruses were taken up by cell bodies rather than terminals or fibers of passage. Our main conclusions arise from data confirmed by both retrograde and anterograde experiments, and as these were strongly consistent with each other and with the literature, we conclude that VTA GABA neurons do indeed make the observed projections. We also observe VGAT+ varicosities or terminals within the regions infused with retrograde tracers, suggestive of synaptic connections in these areas. It remains possible, however, that some retrogradely labeled cells may have resulted from tracer uptake by damaged fibers.

The virus used for anterograde tracing could have spread to adjacent areas such as the rostromedial tegmental nucleus (RMTg), which has been shown in the rat to have overlapping projections with our data (Jhou et al., 2009). In some cases cell bodies in the RMTg were infected with virus (Figure 2). However, this was a very small percentage of the total population of labeled cells, and in our hands very few cells in the RMTg were labeled with retrograde tracers, whereas GABAergic cells were found throughout the VTA.

Another potential concern is the sensitivity of our methods to detect GABAergic or glutamatergic cell bodies in the VTA. Our pilot studies and other labs have shown that

immunohistochemical detection with GAD or GABA antisera in the VTA does not reliably mark cell bodies (Olson and Nestler, 2007; Nair-Roberts et al., 2008). Other approaches to label GABAergic and glutamatergic cell bodies include the use of transgenic mice or *in situ* hybridization (ISH) to label GAD or VGluT2 mRNA. We used GAD67-GFP and VGluT2-IRES-Cre mice to facilitate detection of multiple other markers in the same tissue (TH and retrograde tracers), which may not have been possible with ISH. In GAD67-GFP mice, we observe many retrogradely labeled cells which lack both TH and GFP. This led us to conduct parallel experiments in VGluT2-IRES-Cre mice to label glutamatergic neurons. These experiments reveal retrogradely labeled cells which lacked TH and VGluT2. In both mouse lines, some of these neurons may be false negatives. Importantly, the proportions of retrogradely labeled neurons classified as dopaminergic, GABAergic and glutamatergic are similar between the two lines, indicating that possible false negatives only minimally contribute to our data.

We view the possibility of false negative DA projection neurons as unlikely because the percentage of retrogradely labeled cells positive for TH in our experiments either matched or exceeded those reported the literature, and TH labeling was very consistent across experiments. The GAD67-GFP knock-in line may not label all GABAergic neurons in the VTA. Slight differences in the pattern of Cre-expressing cells in the GAD67-Cre and GAD65-IRES-Cre mouse lines and published ISH studies of GAD isoforms indicate that the two enzymes may be expressed in somewhat distinct cellular populations (Esclapez et al., 1993). GAD65-expressing neurons may therefore account for a proportion of the retrogradely-labeled TH(-)/GFP(-) neurons in GAD67-GFP mice. The results of our retrograde studies in VGluT2-IRES-Cre mice indicate that many of these cells express VGluT2. As we did not label for TH, GAD and VGluT2 in the same tissue, it is possible that our data contain false negatives, but the degree of similarity

between the experiments in the two lines indicates that this cannot entirely account for the observed retrogradely-labeled only neurons.

For labeling of putative glutamatergic neurons we infused a virus expressing Cre-dependent mCherry in VGluT2-IRES-Cre knock-in mice. Cre expression in these mice is restricted to areas containing VGluT2 mRNA (Vong et al., 2011). Our data reveal VGluT2 labeling very consistent with that described by Yamaguchi et al (2011), with a strong mediolateral gradient of expression and substantial overlap with TH immunoreactivity. The large number of cells labeled by the virus indicates we did not likely have many false negative cells. Conversely, there may be cells expressing Cre recombinase that may be of another neurotransmitter phenotype. However, we believe that these do not make up a large portion of our data for several reasons. First, as noted above, we find very high similarity between the results of our retrograde studies using two different transgenic lines to label separate but complementary populations of VTA neurons. Second, we find very similar ratios of neurons projecting to the NAcc as found in the Yamaguchi study. Third, our retrograde studies are consistent with projections recently described using viral-vector mediated anterograde tracing in a different line of VGluT2-Cre mice (Hnasko et al., 2012). The high degree of similarity between our results and studies using other methods, including more traditional ISH labeling of VGluT2 mRNA, suggests that VGluT2-IRES-Cre mice reliably label VGluT2-expressing cells in the VTA.

Comparison to Literature

We describe four classes of VTA projection neurons: TH, TH/VGluT2, GAD, and VGluT2-only expressing cells. The DAergic projections in this study are largely consistent with prior work in rat (Swanson, 1982; Klitenick et al., 1992; Del-Fava et al., 2007). We find higher

ratios of DA neurons in the IF projections to NAcc, amygdala and PFC than has been published. The DA content of the VTA-LHb projection we report is very similar to that described by Swanson, but less than what has been reported in more recent work (Li et al., 1993; Gruber et al., 2007). We also find a higher percentage of DA neurons in the mesocortical projection from all regions of VTA than has been shown previously in rat studies. These discrepancies could be due to species differences between rat and mouse in DA neuron density or projections, or to differential placement of the tracer between studies.

Our experiments confirm and extend recent work describing VGluT2-expressing projection neurons, which includes both TH/VGluT2 and VGluT2-only neurons (Hur and Zaborszky, 2005; Lavin et al., 2005; Yamaguchi et al., 2011; Gorelova et al., 2012; Hnasko et al., 2012). The majority of dopaminergic projections from the paranigral nucleus and nearly all of the dopaminergic neurons projecting to amygdala express VGluT2. Evidence from several groups indicates that VTA TH/VGluT2 neurons projecting to NAcc are capable of releasing both DA and glutamate (Chuhma et al., 2009; Hnasko et al., 2010; Stuber et al., 2010; Tecuapetla et al., 2010). Our data indicate that TH/VGluT2 neurons also project to the amygdala, VP/BNST and MCPO, raising the possibility that co-release of DA and glutamate may occur in these areas. Further studies are necessary to determine the extent and function of co-release in areas other than the striatum.

Previous studies have identified GABAergic projections to the NAcc in rats and mice, to LHb in mice (Van Bockstaele and Pickel, 1995; Brown et al., 2012; van Zessen et al., 2012; Stamatakis et al., 2013), and to PFC, dorsal raphe and VP in rat (Steffensen et al., 1998; Gervasoni et al., 2000; Carr and Sesack, 2000a; Mitrovic and Napier, 2002; Kirouac et al., 2004). VTA glutamate neurons have been shown to project to NAcc and PFC in rats and mice, and to

LHb, amygdala, and VP in mice (Pirot et al., 1992; Yamaguchi et al., 2011; Gorelova et al., 2012; Hnasko et al., 2012). Our data identify more widespread projections to limbic structures for both VTA GABAergic and glutamatergic neurons. The GABAergic projections to MCPO, BNST, LPO, and LH identified here have not been described previously. Unexpectedly, we find that the majority of non-DA VTA projections in mouse express VGluT2 rather than GAD. We confirm that VTA glutamate neurons project to LHb, PFC and NAcc shell and core, and demonstrate that these neurons also project to the amygdala, MCPO/OT, and VP/BNST. Both VTA GABA and glutamatergic neurons make local connections onto both DA and non-DA neurons (Omelchenko and Sesack, 2009; Dobi et al., 2010), but it is not known if these cells also send collaterals outside of the VTA. While GABA neurons comprise 30-35% of the total VTA population, they make up a much smaller percentage of the retrogradely-labeled neurons in this study, which may indicate that a substantial proportion are local interneurons. For both GABA and glutamate neurons, however, it remains unclear whether there are distinct classes of local interneurons and projection neurons.

Our data revealed overall strong similarity between projections using GAD67-Cre and GAD65-IRES-Cre mice, though there were some interesting differences. At the level of the VTA, GAD65-IRES-Cre mice appear to have more Cre-expressing cells than GAD67-Cre mice, though this was not quantified. It is unclear why this may be, but it could be due to differences in GAD isoform expression, as has been suggested in some brain regions (Escalpez et al., 1993), or to differences in the method for generation of the two mouse lines. The GAD65-IRES-Cre line is a knock-in mouse, whereas the GAD67-Cre line is a BAC transgenic. Potential functional implications of these different projections would depend on whether differential Cre expression is truly reflective of differential GAD isoform expression.

Comparison of the GABAergic and glutamatergic projections we observed with known VTA afferent regions reveals that all regions that receive GABAergic and glutamatergic input from the VTA also project back to the VTA (Geisler and Zahm, 2005; Watabe-Uchida et al., 2012). The work of Zahm and colleagues has documented that many of these areas are also interconnected (Geisler and Zahm, 2005). Thus the VTA GABAergic and glutamatergic projections are part of these larger networks, of which only some are shared with the DA projection system. Interestingly, VP, LPO, BNST and LH, which we show receive dense VTA GABA input with relatively less DA input than NAcc, are major sources of afferent input to the VTA (Geisler and Zahm, 2005). Thus VTA non-DA neurons are positioned to provide inhibitory or disinhibitory feedback to the VTA through both local and long-range connections.

Functional Implications

VTA GABA neurons have been implicated in brain stimulation, reward processing, and drug reward, but these studies have largely focused on local intra-VTA mechanisms (Johnson and North, 1992; Klink et al., 2001; Mansvelder and McGehee, 2002; Szabo et al., 2002; Lassen et al., 2007; Cohen et al., 2012; van Zessen et al., 2012; Tolu et al., 2013). Early descriptions of VTA GABAergic projections suggested they might have roles beyond local inhibition (Van Bockstaele and Pickel, 1995; Steffensen et al., 1998; Carr and Sesack, 2000a; 2000b). Our data support the possibility of an expanded role of VTA non-DA neurons in reward processing. We demonstrate non-DA input from the VTA to several regions which support intracranial self-stimulation, intracranial self-administration or place conditioning, including the LPO, LH, VP, and raphe nuclei (Wise, 1996; McBride et al., 1999). The DA projection from VTA to NAcc is critical for reward-related behaviors (Ikemoto, 2010); interestingly, the NAcc projects heavily to

the VP. Thus, VTA GABA and glutamate neurons projecting to VP could influence reward processing downstream of VTA-NAcc DA projections.

Our results indicate that drugs of abuse with primary actions on non-DA neurons may influence VTA GABA, and potentially glutamate, circuits independent of DA neurons. Interestingly, intracranial administration of nicotine into the VTA can have DA-independent behavioral effects (Laviolette and van der Kooy, 2003; Tolu et al., 2013). The GABAergic and glutamatergic circuits from the VTA to downstream limbic regions may be responsible for such effects. VTA GABA and glutamate neurons are therefore positioned to influence both local and network processing of rewarding and reinforcing stimuli (Ikemoto, 2010).

Little is known about what stimuli activate the glutamatergic neurons of the VTA or what functions they may serve, but recent work using optogenetic methods has examined GABAergic projections to the striatum. Brown and colleagues (2012) showed that activation of VTA GABA projections to striatum inhibited cholinergic interneuron activity and enhanced associative learning. Another recent study showed that acute activation of VTA GABA neurons reduced reward consumption (van Zessen et al., 2012). This effect was seen with stimulation of cell bodies in the VTA, but not with stimulation of GABAergic terminals in NAcc. While this may be due to local inhibition of DA neurons (Omelchenko and Sesack, 2009; Tan et al., 2012; Bocklisch et al., 2013), GABAergic projections to regions outside the NAcc may also account for this effect. Our data indicate that the VTA-NAcc projection is one of the more minor VTA GABAergic projections, so it is plausible that other projections also have behavioral significance.

Recent studies in mouse have demonstrated that VTA GABA neurons are activated by aversive stimuli and by reward-predicting cues (Cohen et al., 2012; Tan et al., 2012). Such

stimuli could lead to alterations in VTA DA neuron firing by direct local inhibition as well as indirectly via LHb, NAcc, or VP projections back to VTA. Interestingly, GABA neurons projecting to LHb would have effects opposite that of local inhibition, as the LHb inhibits DA neuron firing via the RMTg (Jhou et al., 2009; Hong et al., 2011). Indeed, release of GABA from VTA-LHb projections results in reward-related behaviors (Stamatakis et al., 2013), whereas activation of GABAergic cell bodies in the VTA can drive aversion (Tan et al., 2012). As mentioned, it is unclear if VTA GABAergic or glutamatergic projections send local collaterals. Our data suggest that VTA GABA and glutamate projection neurons can convey these aversive and reward-related signals independently to several downstream limbic regions involved in appetitive and motivational responses.

Conclusions

We demonstrate that VTA GABA and glutamate neurons project to several forebrain and brainstem structures, many of which do not receive major dopaminergic input. Several of these structures, in turn, are connected with the VTA and with each other, indicating that VTA GABA and glutamate neurons are part of larger networks that have been implicated in reward processing. Future studies genetically targeting VTA GABA or glutamate neurons should take into account these projections as well as local connections.

Acknowledgements

We acknowledge Dr. Yuchio Yanagawa for the GAD67-GFP knock-in mice, Ben Land, Nadia Jordan-Spasov and Samantha Sheppard for help with animals, and Dr. Charles Greer for helpful advice on the manuscript.

Conflict of Interest

The authors have no conflicts of interest to report.

Role of Authors

Study concept and design: S.R.T. and M.R.P. Generation of reagents: S.B., L.M., R.N., R.J.D. Acquisition and interpretation of data: S.R.T. with input from M.R.P. Drafting of manuscript: S.R.T. and M.R.P.

Literature Cited

Bocklisch C, Pascoli V, Wong JC, House DR, Yvon C, de Roo M, Tan KR, Luscher C. 2013. Cocaine disinhibits dopamine neurons by potentiation of GABA transmission in the ventral tegmental area. Science 341(6153):1521-1525.

Brown MT, Tan KR, O'Connor EC, Nikonenko I, Muller D, Luscher C. 2012. Ventral tegmental area GABA projections pause accumbal cholinergic interneurons to enhance associative learning. Nature 492(7429):452-456.

Carr DB, Sesack SR. 2000a. GABA-containing neurons in the rat ventral tegmental area project to the prefrontal cortex. Synapse 38(2):114-123.

Carr DB, Sesack SR. 2000b. Projections from the rat prefrontal cortex to the ventral tegmental area: target specificity in the synaptic associations with mesoaccumbens and mesocortical neurons. The Journal of neuroscience : the official journal of the Society for Neuroscience 20(10):3864-3873.

Chuhma N, Choi WY, Mingote S, Rayport S. 2009. Dopamine neuron glutamate cotransmission: frequency-dependent modulation in the mesoventromedial projection. Neuroscience 164(3):1068-1083.

Cohen JY, Haesler S, Vong L, Lowell BB, Uchida N. 2012. Neuron-type-specific signals for reward and punishment in the ventral tegmental area. Nature 482(7383):85-88.

Del-Fava F, Hasue RH, Ferreira JG, Shammah-Lagnado SJ. 2007. Efferent connections of the rostral linear nucleus of the ventral tegmental area in the rat. Neuroscience 145(3):1059-1076.

Di Chiara G, Imperato A. 1988. Drugs abused by humans preferentially increase synaptic dopamine concentrations in the mesolimbic system of freely moving rats. Proceedings of the National Academy of Sciences of the United States of America 85(14):5274-5278.

Dobi A, Margolis EB, Wang HL, Harvey BK, Morales M. 2010. Glutamatergic and nonglutamatergic neurons of the ventral tegmental area establish local synaptic contacts with dopaminergic and nondopaminergic neurons. The Journal of neuroscience : the official journal of the Society for Neuroscience 30(1):218-229.

Esclapez M, Tillakaratne NJ, Tobin AJ, Houser CR. 1993. Comparative localization of mRNAs encoding two forms of glutamic acid decarboxylase with nonradioactive in situ hybridization methods. The Journal of comparative neurology 331(3):339-362.

Fields HL, Hjelmstad GO, Margolis EB, Nicola SM. 2007. Ventral tegmental area neurons in learned appetitive behavior and positive reinforcement. Annual review of neuroscience 30:289-316.

Geisler S, Zahm DS. 2005. Afferents of the ventral tegmental area in the rat-anatomical substratum for integrative functions. The Journal of comparative neurology 490(3):270-294.

Gervasoni D, Peyron C, Rampon C, Barbagli B, Chouvet G, Urbain N, Fort P, Luppi PH. 2000. Role and origin of the GABAergic innervation of dorsal raphe serotonergic neurons. The Journal of neuroscience : the official journal of the Society for Neuroscience 20(11):4217-4225.

Gorelova N, Mulholland PJ, Chandler LJ, Seamans JK. 2012. The glutamatergic component of the mesocortical pathway emanating from different subregions of the ventral midbrain. Cerebral cortex 22(2):327-336.

Gruber C, Kahl A, Lebenheim L, Kowski A, Dittgen A, Veh RW. 2007. Dopaminergic projections from the VTA substantially contribute to the mesohabenular pathway in the rat. Neuroscience letters 427(3):165-170.

Hnasko TS, Chuhma N, Zhang H, Goh GY, Sulzer D, Palmiter RD, Rayport S, Edwards RH. 2010. Vesicular glutamate transport promotes dopamine storage and glutamate corelease in vivo. Neuron 65(5):643-656.

Hnasko TS, Hjelmstad GO, Fields HL, Edwards RH. 2012. Ventral tegmental area glutamate neurons: electrophysiological properties and projections. The Journal of neuroscience : the official journal of the Society for Neuroscience 32(43):15076-15085.

Hong S, Jhou TC, Smith M, Saleem KS, Hikosaka O. 2011. Negative reward signals from the lateral habenula to dopamine neurons are mediated by rostromedial tegmental nucleus in primates. The Journal of neuroscience : the official journal of the Society for Neuroscience 31(32):11457-11471.

Hur EE, Zaborszky L. 2005. Vglut2 afferents to the medial prefrontal and primary somatosensory cortices: a combined retrograde tracing in situ hybridization study [corrected]. The Journal of comparative neurology 483(3):351-373.

Ikemoto S. 2010. Brain reward circuitry beyond the mesolimbic dopamine system: a neurobiological theory. Neuroscience and biobehavioral reviews 35(2):129-150.

Jhou TC, Geisler S, Marinelli M, Degarmo BA, Zahm DS. 2009. The mesopontine rostromedial tegmental nucleus: A structure targeted by the lateral habenula that projects to the ventral tegmental area of Tsai and substantia nigra compacta. The Journal of comparative neurology 513(6):566-596.

Johnson SW, North RA. 1992. Opioids excite dopamine neurons by hyperpolarization of local interneurons. The Journal of neuroscience : the official journal of the Society for Neuroscience 12(2):483-488.

Kawano M, Kawasaki A, Sakata-Haga H, Fukui Y, Kawano H, Nogami H, Hisano S. 2006. Particular subpopulations of midbrain and hypothalamic dopamine neurons express vesicular glutamate transporter 2 in the rat brain. The Journal of comparative neurology 498(5):581-592.

Kirouac GJ, Li S, Mabrouk G. 2004. GABAergic projection from the ventral tegmental area and substantia nigra to the periaqueductal gray region and the dorsal raphe nucleus. The Journal of comparative neurology 469(2):170-184.

Klink R, de Kerchove d'Exaerde A, Zoli M, Changeux JP. 2001. Molecular and physiological diversity of nicotinic acetylcholine receptors in the midbrain dopaminergic nuclei. The Journal of neuroscience : the official journal of the Society for Neuroscience 21(5):1452-1463.

Klitenick MA, Deutch AY, Churchill L, Kalivas PW. 1992. Topography and functional role of dopaminergic projections from the ventral mesencephalic tegmentum to the ventral pallidum. Neuroscience 50(2):371-386.

Lammel S, Hetzel A, Hackel O, Jones I, Liss B, Roeper J. 2008. Unique properties of mesoprefrontal neurons within a dual mesocorticolimbic dopamine system. Neuron 57(5):760-773.

Lammel S, Ion DI, Roeper J, Malenka RC. 2011. Projection-specific modulation of dopamine neuron synapses by aversive and rewarding stimuli. Neuron 70(5):855-862.

Lassen MB, Brown JE, Stobbs SH, Gunderson SH, Maes L, Valenzuela CF, Ray AP, Henriksen SJ, Steffensen SC. 2007. Brain stimulation reward is integrated by a network of electrically coupled GABA neurons. Brain research 1156:46-58.

Lavin A, Nogueira L, Lapish CC, Wightman RM, Phillips PE, Seamans JK. 2005. Mesocortical dopamine neurons operate in distinct temporal domains using multimodal signaling. The Journal of neuroscience : the official journal of the Society for Neuroscience 25(20):5013-5023.

Laviolette SR, Alexson TO, van der Kooy D. 2002. Lesions of the tegmental pedunculopontine nucleus block the rewarding effects and reveal the aversive effects of nicotine in the ventral tegmental area. The Journal of neuroscience : the official journal of the Society for Neuroscience 22(19):8653-8660.

Laviolette SR, van der Kooy D. 2003. Blockade of mesolimbic dopamine transmission dramatically increases sensitivity to the rewarding effects of nicotine in the ventral tegmental area. Molecular psychiatry 8(1):50-59, 59.

Li YQ, Takada M, Shinonaga Y, Mizuno N. 1993. The sites of origin of dopaminergic afferent fibers to the lateral habenular nucleus in the rat. The Journal of comparative neurology 333(1):118-133.

Mansvelder HD, McGehee DS. 2002. Cellular and synaptic mechanisms of nicotine addiction. Journal of neurobiology 53(4):606-617.

McBride WJ, Murphy JM, Ikemoto S. 1999. Localization of brain reinforcement mechanisms: intracranial self-administration and intracranial place-conditioning studies. Behavioural brain research 101(2):129-152.

Mitrovic I, Napier TC. 2002. Mu and kappa opioid agonists modulate ventral tegmental area input to the ventral pallidum. The European journal of neuroscience 15(2):257-268.

Nair-Roberts RG, Chatelain-Badie SD, Benson E, White-Cooper H, Bolam JP, Ungless MA. 2008. Stereological estimates of dopaminergic, GABAergic and glutamatergic neurons in the ventral tegmental area, substantia nigra and retrorubral field in the rat. Neuroscience 152(4):1024-1031.

Ohtsuka N, Badurek S, Busslinger M, Benes FM, Minichiello L, Rudolph U. 2013. GABAergic neurons regulate lateral ventricular development via transcription factor Pax5. Genesis 51(4):234-245.

Olson VG, Nestler EJ. 2007. Topographical organization of GABAergic neurons within the ventral tegmental area of the rat. Synapse 61(2):87-95.

Omelchenko N, Sesack SR. 2009. Ultrastructural analysis of local collaterals of rat ventral tegmental area neurons: GABA phenotype and synapses onto dopamine and GABA cells. Synapse 63(10):895-906.

Paxinos G, Franklin KBJ, Franklin KBJ. 2001. The mouse brain in stereotaxic coordinates. San Diego: Academic Press.

Pirot S, Godbout R, Mantz J, Tassin JP, Glowinski J, Thierry AM. 1992. Inhibitory effects of ventral tegmental area stimulation on the activity of prefrontal cortical neurons: evidence for the involvement of both dopaminergic and GABAergic components. Neuroscience 49(4):857-865.

Stamatakis AM, Jennings JH, Ung RL, Blair GA, Weinberg RJ, Neve RL, Boyce F, Mattis J, Ramakrishnan C, Deisseroth K, Stuber GD. 2013. A unique population of ventral

tegmental area neurons inhibits the lateral habenula to promote reward. Neuron 80(4):1039-1053.

Steffensen SC, Svingos AL, Pickel VM, Henriksen SJ. 1998. Electrophysiological characterization of GABAergic neurons in the ventral tegmental area. The Journal of neuroscience : the official journal of the Society for Neuroscience 18(19):8003-8015.

Stuber GD, Hnasko TS, Britt JP, Edwards RH, Bonci A. 2010. Dopaminergic terminals in the nucleus accumbens but not the dorsal striatum corelease glutamate. The Journal of neuroscience : the official journal of the Society for Neuroscience 30(24):8229-8233.

Swanson LW. 1982. The projections of the ventral tegmental area and adjacent regions: a combined fluorescent retrograde tracer and immunofluorescence study in the rat. Brain research bulletin 9(1-6):321-353.

Szabo B, Siemes S, Wallmichrath I. 2002. Inhibition of GABAergic neurotransmission in the ventral tegmental area by cannabinoids. The European journal of neuroscience 15(12):2057-2061.

Tamamaki N, Yanagawa Y, Tomioka R, Miyazaki J, Obata K, Kaneko T. 2003. Green fluorescent protein expression and colocalization with calretinin, parvalbumin, and somatostatin in the GAD67-GFP knock-in mouse. The Journal of comparative neurology 467(1):60-79.

Tan KR, Brown M, Labouebe G, Yvon C, Creton C, Fritschy JM, Rudolph U, Luscher C. 2010. Neural bases for addictive properties of benzodiazepines. Nature 463(7282):769-774.

Tan KR, Yvon C, Turiault M, Mirzabekov JJ, Doehner J, Labouebe G, Deisseroth K, Tye KM, Luscher C. 2012. GABA neurons of the VTA drive conditioned place aversion. Neuron 73(6):1173-1183.

Tecuapetla F, Patel JC, Xenias H, English D, Tadros I, Shah F, Berlin J, Deisseroth K, Rice ME, Tepper JM, Koos T. 2010. Glutamatergic signaling by mesolimbic dopamine neurons in the nucleus accumbens. The Journal of neuroscience : the official journal of the Society for Neuroscience 30(20):7105-7110.

Tolu S, Eddine R, Marti F, David V, Graupner M, Pons S, Baudonnat M, Husson M, Besson M, Reperant C, Zemdegs J, Pages C, Hay YA, Lambolez B, Caboche J, Gutkin B, Gardier AM, Changeux JP, Faure P, Maskos U. 2013. Co-activation of VTA DA and GABA neurons mediates nicotine reinforcement. Molecular psychiatry 18(3):382-393.

Van Bockstaele EJ, Pickel VM. 1995. GABA-containing neurons in the ventral tegmental area project to the nucleus accumbens in rat brain. Brain research 682(1-2):215-221.

van Zessen R, Phillips JL, Budygin EA, Stuber GD. 2012. Activation of VTA GABA neurons disrupts reward consumption. Neuron 73(6):1184-1194.

Vong L, Ye C, Yang Z, Choi B, Chua S, Jr., Lowell BB. 2011. Leptin action on GABAergic neurons prevents obesity and reduces inhibitory tone to POMC neurons. Neuron 71(1):142-154.

Wang X, Sun QQ. 2012. Characterization of axo-axonic synapses in the piriform cortex of Mus musculus. The Journal of comparative neurology 520(4):832-847.

Watabe-Uchida M, Zhu L, Ogawa SK, Vamanrao A, Uchida N. 2012. Whole-brain mapping of direct inputs to midbrain dopamine neurons. Neuron 74(5):858-873.

Wise RA. 1996. Addictive drugs and brain stimulation reward. Annual review of neuroscience 19:319-340.

Yamaguchi T, Sheen W, Morales M. 2007. Glutamatergic neurons are present in the rat ventral tegmental area. The European journal of neuroscience 25(1):106-118.

Yamaguchi T, Wang HL, Li X, Ng TH, Morales M. 2011. Mesocorticolimbic glutamatergic pathway. The Journal of neuroscience : the official journal of the Society for Neuroscience 31(23):8476-8490.

Figure Legends

Table of Abbreviations Used in Figures

ac	anterior commissure
BLA	basolateral amygdalar nucleus
BNST	bed nucleus of the stria terminalis
CeA	central amygdalar nucleus
ChAT	choline acetyltransferase
ChR2-YFP	channelrhodopsin fused to yellow fluorescent protein
Cli	caudal linear nucleus
DpMe	deep mesencephalic nucleus
DR	dorsal raphe nucleus
DRC	dorsal raphe nucleus, caudal part
ECIC	external cortex of the inferior colliculus
FG	fluorogold
fr	fasciculus retroflexus
GAD65	glutamic acid decarboxylase, 65 kDa isoform
GAD67	glutamic acid decarboxylase, 67 kDa isoform
GFP	green fluorescent protein
HDB	horizontal limb of the diagonal band of Broca
ICjM	islands of Calleja, major island
IF	interfascicular nucleus
IL	infralimbic cortex
LSV	lateral septal nucleus, ventral part
MCPO	magnocellular preoptic nucleus
MDM	mediodorsal thalamic nucleus, medial part
mfb	medial forebrain bundle
MHb	medial habenula
MnR	median raphe nucleus
MS	medial septum
NAcc	nucleus accumbens
PAG	periaqueductal gray
PBP	parabrachial pigmented nucleus
PFC	prefrontal cortex
PMnR	paramedian raphe nucleus
PN	paranigral nucleus
PnC	pontine reticular nucleus, caudal part
PPTg	pedunculopontine tegmental nucleus
PreL	prelimbic cortex
PV	paraventricular thalamic nucleus
RC	raphe cap
Rli	rostral linear nucleus
RN	red nucleus

IMD	intermediodorsal thalamic nucleus
IPAC	interstitial nucleus of the posterior limb of the anterior commissure
IPN	interpeduncular nucleus
LDTg	laterodorsal tegmental nucleus
LH	lateral hypothalamus
LHb	lateral habenula
LPO	lateral preoptic area
SI	substantia innomata
SNc	substantia nigra, pars compacta
SNr	substantia nigra, pars reticulata
TH	tyrosine hydroxylase
VGAT	vesicular GABA transporter
VP	ventral pallidum
VTA	ventral tegmental area

Figure 1. GAD-Cre animals allow for cell-specific anterograde tracing. Infusion of AAV-Ef1a-DIO-mCherry permits visualization of Cre-expressing cells in the ventral tegmental area (VTA; panels A, E). Many Cre-expressing cells in GAD67-Cre (A-D) and GAD65-IRES-Cre mice (E-H) clearly stain for GAD67 and lack tyrosine hydroxylase, a marker of dopamine neurons (white arrows). GABAergic Cre+ cells are present throughout the subregions of the VTA (Panel I). J) An example infusion site for anterograde tracing demonstrating labeling centered in the VTA (Case S2, used for Figures 3 and 5) Scale bars in panels D, H, I = 50 μm, in panel J = 200 μm.

Figure 2. Injection sites for five cases (three restricted almost entirely to VTA, two control infusions) of viral infusion into GAD-Cre animals for anterograde tracing. Coronal drawings from rostral (top) to caudal VTA (bottom) depict the spread of virus (as detected by transduced cell bodies). Each dot represents an eYFP-expressing cell body transduced by the virus. Cases GC 152, 153, and 116 are GAD67-Cre mice, and Cases S2 and S3 are GAD65-IRES-Cre mice. In case GC 152, the infusion was restricted to the red nucleus, dorsal to the VTA, and in case GC 116 the infusion was centered in the interpeduncular nucleus, ventral to the VTA.

Figure 3. Panels showing anterograde labeled GABAergic fibers from case S2, which had an infusion of virus driving channelrhodopsin-eYFP, stained for eYFP (green) and TH (magenta). Panels A, D, G, and J show diagrams of forebrain sections containing labeled fibers. Black boxes indicate the regions shown in B, E, H, and K. Panels C, F, I, and L differ from B, D, F, and H only in the addition of the TH channel to delineate brain regions. Inset in Panel E shows the varicose nature of the fibers in surrounding the island of Calleja (scale bar = 10 μm). Note

the largely non-overlapping patterns of GABAergic fibers and TH labeling. Scale bars in in C, F, I, L = 100 μm.

Figure 4. Coronal diagrams of line drawings of labeled fibers in representative cases from similar levels in both GAD65-IRES-Cre mice (Case S3; A, C, E, G, I, K, M, O) and GAD67-Cre mice (Case GC 153; B, D, F, H, J, L, N, P).

Figure 5. Panels showing images from more caudal areas of case S2 stained for channelrhodopsin-eYFP (green), TH (magenta) and ChAT (blue). Panels B, E, H, and K are enlargements of the areas outlined in A, D, G and J, respectively. Scale bars = 100 μm.

Figure 6. VTA GABA neurons surround cholinergic and non-cholinergic neurons. A) Low magnification projection image depicting GABAergic fibers apposing cholinergic cellular profiles (white arrowheads) and non-cholinergic regions (white arrows) in NAcc core (from case S2). B) High magnification projection image of outlined region in panel A. Note how the labeled fibers follow the proximal dendrites and contain several varicosities that appose the cell body and dendrites of cholinergic neurons. C) Triple labeling in NAcc shell for fibers, cholinergic cells and NeuN to reveal all neuronal nuclei suggest that GABA fibers may make similar appositions and encapsulations around non-cholinergic cells (white arrow, see white arrows in panel A). D) Co-localization of YFP+ varicosities and boutons with immunolabeling of the vesicular GABA transporter, which is localized to inhibitory synapses, indicates that these fibers are indeed GABAergic and make inhibitory connections. This image is from the lateral habenula (LHb) of case S2. Similar co-labeling with VGAT is seen in LHb, CeA, VP, NAcc and

VTA of both GAD67-Cre and GAD65-IRES-Cre mice. Orthogonal views are of the bouton nearest the scale bar in lower right. Scale bars in A = 50 μm; B, C = 10 μm; D = 5 μm.

Figure 7. Retrograde tracing in GAD67-GFP knock-in mice. A-D) GFP+ cells in the VTA show immunohistochemical markers of GABA neurons (white arrows). Most, but not all GFP+ neurons (black arrowheads), clearly stain for GAD67 and lack TH immunoreactivity. Some are at the same level as surrounding neuropil. E-H) Injection of FluoroGold (FG) into the magnocellular preoptic nucleus revealed three classes of VTA projections: FG/TH (dopaminergic), FG/GFP (white arrowheads, GABAergic) and FG+ only (black arrows, TH- and GFP-; non-DA, non-GABA). I) Injections of Red Retrobeads gave similar results (white arrowhead shows a GFP+/retrogradely labeled cell, black arrow a non-TH/non-GFP/retrogradely labeled cell), here from an injection into central amygdala. J-K) Images of injections of Retrobeads (J) or FG (K) centered in LHb display spread of injection. Scale bars in D = 50 μm; in H, I = 20 μm; in J, K = 100 μm.

Figure 8. Diagrams of infusion sites of retrograde tracers. Tracers were infused into seven locations in GAD67-GFP knock-in mice to verify GABAergic projections. The center and spread of the tracer of a representative infusion for each target area are indicated by the filled and shaded regions, respectively. Some infusions had some minor overlap with adjacent regions.

Figure 9. Coronal diagrams from rostral to caudal (A, C, E, G, I) levels of the VTA showing the location of GABA projection neurons by retrograde tracing. Panels A, C, E, G and I display cells from representative cases of infusions of tracer into NAcc Shell (filled circles), NAcc Core

(filled squares), mPFC (filled triangles) and amygdala (filled diamonds). Panels B, D, F, H, and J display mark cells from cases of tracer infused into LHb (open circles), VP/BNST (open squares) and MCPO/OT (open triangles). The majority of retrogradely labeled VTA GABA neurons are found in the lateral and ventral regions of the VTA.

Figure 10. Graphs indicating the percentage of retrogradely labeled cells within each VTA subregion by infusion target by neurotransmitter phenotype. Panels in the left column (A, C, E, G, I) contain data from GAD67-GFP mice. Panels in the right column (B, D, F, H, J) contain data from VGluT2-IRES-Cre mice. The average number of retrogradely labeled cells per animal is contained in each column. Black indicates the percentage co-labeled for TH, black with gray stripes indicates the percentage labeled with TH and VGluT2 (VGluT2-IRES-Cre mice), gray is the percentage co-labeled for GFP (in GAD67-GFP mice) or negative for TH and VGluT2 (in VGluT2-IRES-Cre mice), and white is the percentage labeled for VGluT2 only (VGluT2-IRES-Cre mice) or negative for both TH and GFP (GAD67-GFP mice).

Figure 11. Retrograde tracing in VGluT2-IRES-Cre mice. Infusion of FG into MCPO (A-D) or LHb (E-H) and AAV-DIO-Ef1a-mCherry into the VTA revealed several types of projections: FG/TH only, FG/TH/VGluT2 (black arrowheads), FG/VGluT2 only (black arrows), and FG only (white arrowheads). Panels A-D show cells in the interfascicular nucleus, and panels E-H are from the parabrachial pigmented nucleus. Scale bars = 20 μm.

Figure 12. Coronal diagrams from rostral to caudal (top to bottom) levels of VTA showing the location of retrogradely labeled VGluT2-only neurons. One representative case from each

injection site was mapped to demonstrate the location of projection neurons throughout the rostral-caudal axis of the VTA. TH+/retrogradely labeled cells were not depicted for clarity and to emphasize the non-dopaminergic projections. Note the majority of VGluT2-only projections originate from the medial nuclei (RLi and IF) and the medial portions of PBP and PN.

Figure 13. Summary diagram of VTA GABAergic (Panel A) and glutamatergic (Panel B) efferents. The thickness of the arrows roughly depicts the density of the projection.

Table 1. Viruses used for identification and tracing of GABAergic neurons

Virus	Purpose	Amount	Source
AAV-Ef1a-DIO-hChR2-eYFP	Label axonal projections	0.2-0.3 µl; unilateral	UNC Vector Core
AAV-Ef1a-DIO-hChR2-mCherry	Label axonal projections	0.2-0.3 µl; unilateral	UNC Vector Core
AAV-Ef1a-DIO-mCherry	Label cell bodies in infusion site	0.5 µl; unilateral	UNC Vector Core
AAV-Ef1a-DIO-Syb2-GFP	Enrich labeling in synaptic terminals	0.2 µl; unilateral	Ralph DiLeone

AAV – adeno-associated virus; EF1a- elongation factor 1a promoter; DIO – double floxed inverse open reading frame; hChR2 - channelrhodopsin

Table 2. Primary Antibodies

Antibody Name	Immunogen	Manufacturer	Host	Clonality	Dilution
TH	Denatured TH from rat pheochromocytoma (SDS)	Millipore; AB152	Rabbit	Polyclonal	1:1000
TH	Native TH from rat pheochromocytoma	Millipore; AB1542, Lot# NG1861500	Sheep	Polyclonal	1:1000
TH	Two synthetic peptides; one from amino acids 1-100 of mouse tyrosine hydroxylase, one from amino acids 398-498 of mouse tyrosine hydroxylase	Pierce; PA1-46351	Chicken	Polyclonal	1:1000
GFP	Recombinant full length protein (eGFP)	Abcam; ab13970	Chicken	Polyclonal	1:1500
Choline Acetyltransferase (ChAT)	Human placental Choline acetyltransferase	Chemicon; AB144P	Goat	Polyclonal	1:500
dsRed	Full-length dsRed-Express	ClonTech; 632496	Rabbit	Polyclonal	1:500
VGAT	Synthetic 17 amino acid peptide - VHSLEGLIEAYRTNAED - corresponding to C terminus of rat VGAT	Millipore; AB5602P	Rabbit	Polyclonal	1:1000
VGluT2	Recombinant GST-tagged VGluT2	Millipore; AB2251	Guinea Pig	Polyclonal	1:500
Substance P	Synthetic Substance P coupled to KLH with Carbodiimide	ImmunoStar	Rabbit	Polyclonal	1:500
FluoroGold	FluoroGold	FluoroChrome	Rabbit	Polyclonal	1:500
GAD67	Synthetic peptide - C-PDSPQRREKLHK corresponding to amino acids 526-537 of human GAD67	Abcam; ab80589	Goat	Polyclonal	1:500

Table 3. Relative Density of GABAergic Fibers in Various Brain Structures After AAV-Ef1a-DIO-ChR2-eYFP Injection into the VTA from Several Cases.

	GAD65-IRES-Cre			GAD67-Cre		
Brain Structure	S2	S3	S4	GC 120	GC 122	GC 153
Cortex						
Prelimbic	+			+	+	+
Infralimbic	+			+		
Dorsal peduncular	+	+	+	+	+	+
Dorsal tenia tecta	+			+		+
Piriform				++	+	+
Claustrum				+		
Endopiriform Nucleus				++	+	
Striatum						
Nucleus Accumbens Shell	+	+	+	+	+	+
Nucleus Accumbens Core	+	+	+	+		
Major Island of Calleja	++	+	+	++	++	++
Caudate/Putamen	+	+	+	+	+	
Olfactory Tubercle		+	+			
Ventral Pallidum	++++	++	+	++++	+++	++++
Substantia Innominata	++	+			+	+
Septum						
Lateral Septum, dorsal						
Lateral Septum, intermediate	+	+		+	+	++
Medial Septum	+		+	+	+	+
Diagonal Band of Broca	+	+	+	+	++	++
Bed Nucleus of Stria Terminalis	+++	+++	+	++	+	+
Interstitial Nucleus of Posterior Anterior Commissure	++	++			+	+
Hypothalamus						
Medial preoptic area	++	+				+
Lateral preoptic area	+++	++	+	++	+	++
Magnocellular preoptic area	+	+	+	+++	++	+++
Lateral hypothalamic area	++++	+++	++	+++	+++	+++
Dorsomedial hypothalamic area	+	+	+	+	+	+
Lateral Globus Pallidus	+	+	+	+		
Thalamus/epithalamus						
Paratenial thalamic nucleus	+					+
Paraventricular thalamic nucleus	+	+		+		
Ventromedial thalamic nucleus				+		
Mediodorsal thalamic nucleus	+					
Intermediodorsal thalamic nucleus	+	+				
Lateral habenula	++	++	+	+++	++	++
Reticular thalamic nucleus		+				
Central medial thalamic nucleus		+	+	+	+	+
Parafascicular thalamic nucleus	+	++	++			
Zona Incerta	+++		+			+
Sublenticular extended amygdala	+	++	+	++	+	++
Amygdala						
Central amygdala	+++	++	+	+	+	+
Basolateral amygdala	+					
Basomedial amygdala	+	+		+	+	+
Midbrain						
Superior Colliculus		++		+	++	+
Periaqueductal Gray	++	+		+	+	
Substantia Nigra	+	+	+	+	+	+
Deep Mesencephalic Nucleus	+	+	+	+	++	+
Retrorubral Field	+	+	+	++	++	++
Pons and Medulla						
Dorsal Raphe	+++	++	+	++	+	++
Raphe Cap	+	+				+
Median Raphe	++	+	+	+	++	+
Paramedian Raphe	+			+	+	+
Anterior tegmental nucleus	+			+	+	+
Pedunculopontine nucleus	+		+	+	+	+
Laterodorsal tegmental nucleus	+	+	+	+	+	+
Locus Coeruleus	+	+			+	+
Supraoculomotor Nucleus	+		+	+	+	+
External cortex of inferior colliculus		+	+			
Medioventral periolivary nucleus		+		+		
Lateral parabrachial nucleus	+	+	+		+	+

Table 4. Percentage of retrogradely-labeled cells in VGluT2-IRES-Cre mice according to putative neurotransmitter phenotype.

VTA Subnucleus	Retrograde Infusion	FG/TH	FG/TH/VGluT2	FG/VGluT2	FG/TH(-)/ VGluT2(-)	n[a]
Rli	NAcc Shell	43%	14%	0%	43%	3.5
	NAcc Core	10%	0%	60%	30%	5
	LHb	0%	4%	69%	27%	26
	VP	17%	10%	49%	23%	132
	PFC	13%	6%	35%	45%	15.5
	Amyg	0%	58%	17%	25%	6
	MCPO	1%	3%	87%	8%	103.5
If	NAcc Shell	51%	25%	5%	18%	38
	NAcc Core	29%	26%	40%	6%	17.5
	LHb	0%	0%	78%	22%	29
	VP	9%	26%	60%	5%	93
	PFC	6%	6%	31%	56%	8
	Amyg	-	-	-	-	0
	MCPO	2%	12%	80%	6%	25.5
PBP	NAcc Shell	54%	28%	12%	6%	108.5
	NAcc Core	43%	29%	15%	13%	78.5
	LHb	8%	1%	69%	22%	37
	VP	45%	18%	18%	19%	297
	PFC	59%	15%	15%	11%	69.5
	Amyg	15%	60%	12%	13%	54
	MCPO	40%	22%	23%	16%	186
PN	NAcc Shell	38%	52%	4%	5%	45.5
	NAcc Core	35%	43%	16%	5%	18.5
	LHb	0%	0%	0%	100%	1
	VP	20%	53%	22%	5%	99
	PFC	14%	71%	10%	5%	10.5
	Amyg	0%	81%	13%	6%	8
	MCPO	12%	79%	6%	3%	16.5
Cli	NAcc Shell	94%	0%	0%	6%	8.5
	NAcc Core	36%	36%	11%	18%	14
	LHb	0%	0%	55%	45%	5.5
	VP	35%	16%	6%	43%	51
	PFC	85%	8%	0%	8%	6.5
	Amyg	8%	85%	0%	8%	6.5
	MCPO	11%	69%	6%	14%	18

n[a] = average number of total retrogradely labeled cells from two animals per infusion region. These numbers were used to calculate the percentages listed.

Table 5. Percentage of VTA cell types containing retrograde tracers (FluoroGold or Retrobeads)

VTA Subregion	Retrograde Infusion	Percent of GFP+ neurons with tracer	Percent of TH only neurons with tracer	Percent of TH/VGluT2 neurons with tracer	Percent of VGluT2 only neurons with tracer
Rli	NAcc Shell	0%	13%	14%	0%
	NAcc Core	0%	11%	0%	1%
	LHb	2%	0%	5%	7%
	VP/BNST	15%	47%	33%	26%
	PFC	0%	9%	15%	3%
	Amyg	0%	0%	18%	0%
	MCPO/OT	9%	18%	10%	33%
If	NAcc Shell	14%	58%	51%	1%
	NAcc Core	0%	56%	20%	4%
	LHb	5%	0%	0%	15%
	VP/BNST	9%	80%	55%	35%
	PFC	0%	2%	3%	2%
	Amyg	0%	0%	0%	0%
	MCPO.OT	0%	14%	7%	12%
PBP	NAcc Shell	4%	25%	32%	4%
	NAcc Core	1%	18%	22%	4%
	LHb	10%	1%	0%	9%
	VP/BNST	18%	38%	40%	24%
	PFC	2%	12%	11%	5%
	Amyg	3%	2%	18%	2%
	MCPO/OT	12%	24%	34%	18%
PN	NAcc Shell	4%	42%	58%	5%
	NAcc Core	1%	33%	19%	5%
	LHb	6%	0%	0%	0%
	VP/BNST	13%	77%	74%	37%
	PFC	3%	3%	15%	2%
	Amyg	3%	0%	8%	2%
	MCPO/OT	2%	12%	28%	3%
Cli	NAcc Shell	3%	28%	0%	0%
	NAcc Core	0%	20%	29%	7%
	LHb	7%	0%	0%	12%
	VP/BNST	3%	44%	67%	30%
	PFC	0%	13%	3%	0%
	Amyg	0%	1%	16%	0%
	MCPO/OT	1%	6%	25%	4%

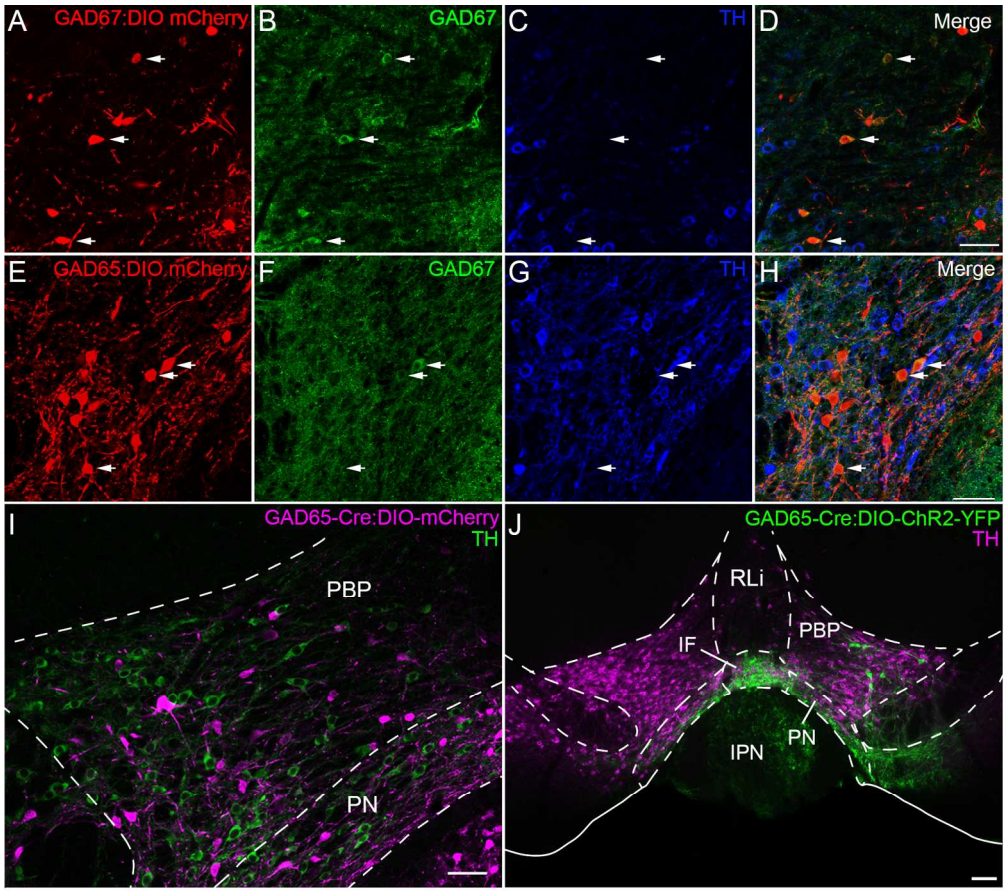

Figure 1. GAD-Cre animals allow for cell-specific anterograde tracing. Infusion of AAV-Ef1a-DIO-mCherry permits visualization of Cre-expressing cells in the ventral tegmental area (VTA; panels A, E). Many Cre-expressing cells in GAD67-Cre (A-D) and GAD65-IRES-Cre mice (E-H) clearly stain for GAD67 and lack tyrosine hydroxylase, a marker of dopamine neurons (white arrows). GABAergic Cre+ cells are present throughout the subregions of the VTA (Panel I). J) An example infusion site for anterograde tracing demonstrating labeling centered in the VTA (Case S2, used for Figures 3 and 5) Scale bars in panels D, H, I = 50 μm, in panel J = 200 μm.
171x152mm (300 x 300 DPI)

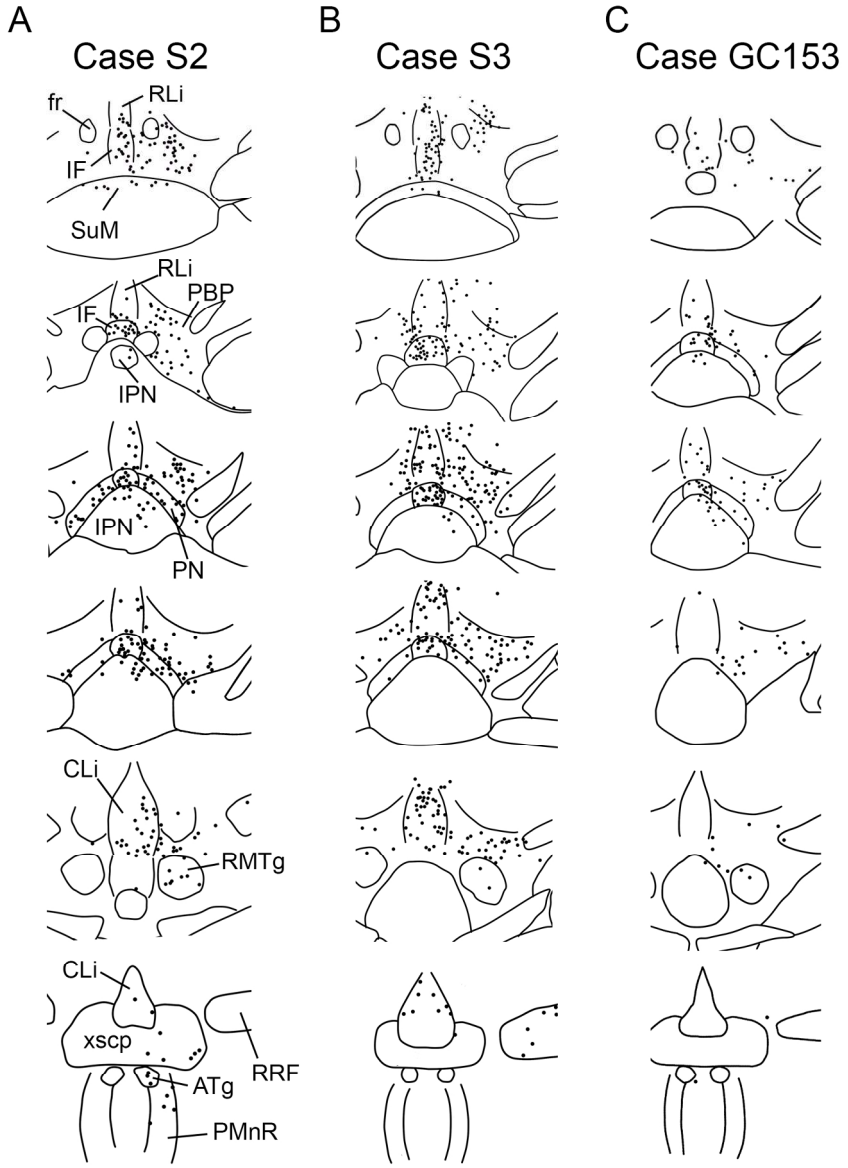

Figure 2. Injection sites for five cases (three restricted almost entirely to VTA, two control infusions) of viral infusion into GAD-Cre animals for anterograde tracing. Coronal drawings from rostral (top) to caudal VTA (bottom) depict the spread of virus (as detected by transduced cell bodies). Each dot represents an eYFP-expressing cell body transduced by the virus. Cases GC 152, 153, and 116 are GAD67-Cre mice, and Cases S2 and S3 are GAD65-IRES-Cre mice. In case GC 152, the infusion was restricted to the red nucleus, dorsal to the VTA, and in case GC 116 the infusion was centered in the interpeduncular nucleus, ventral to the VTA.
165x214mm (300 x 300 DPI)

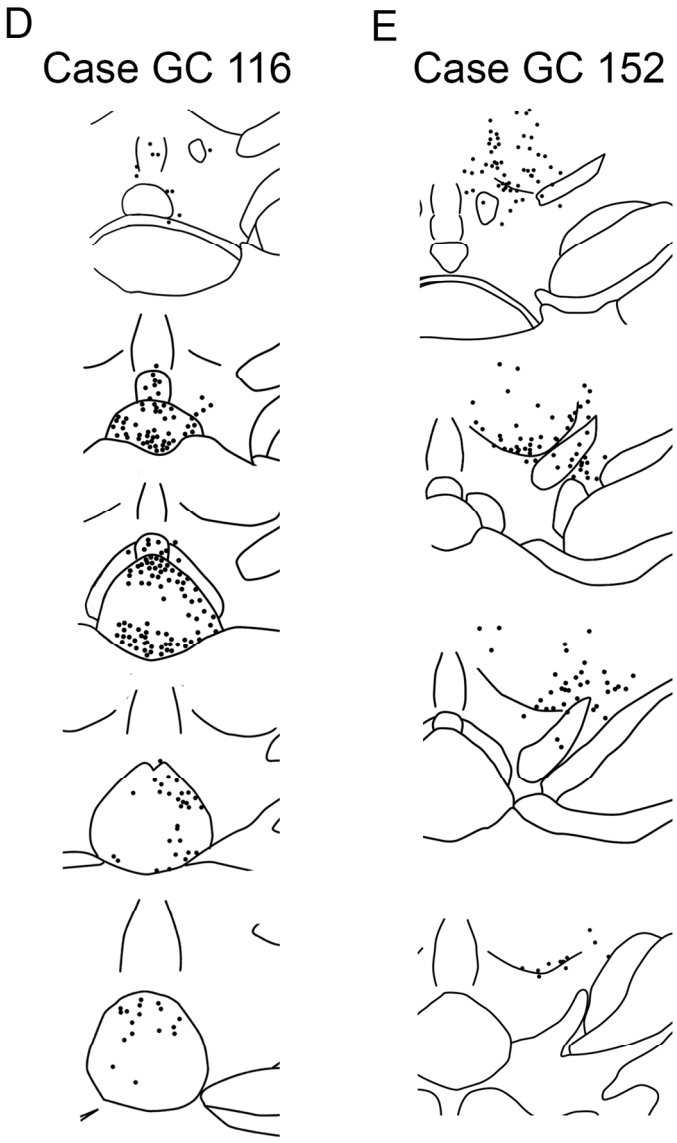

Figure 2 plate 2
118x182mm (300 x 300 DPI)

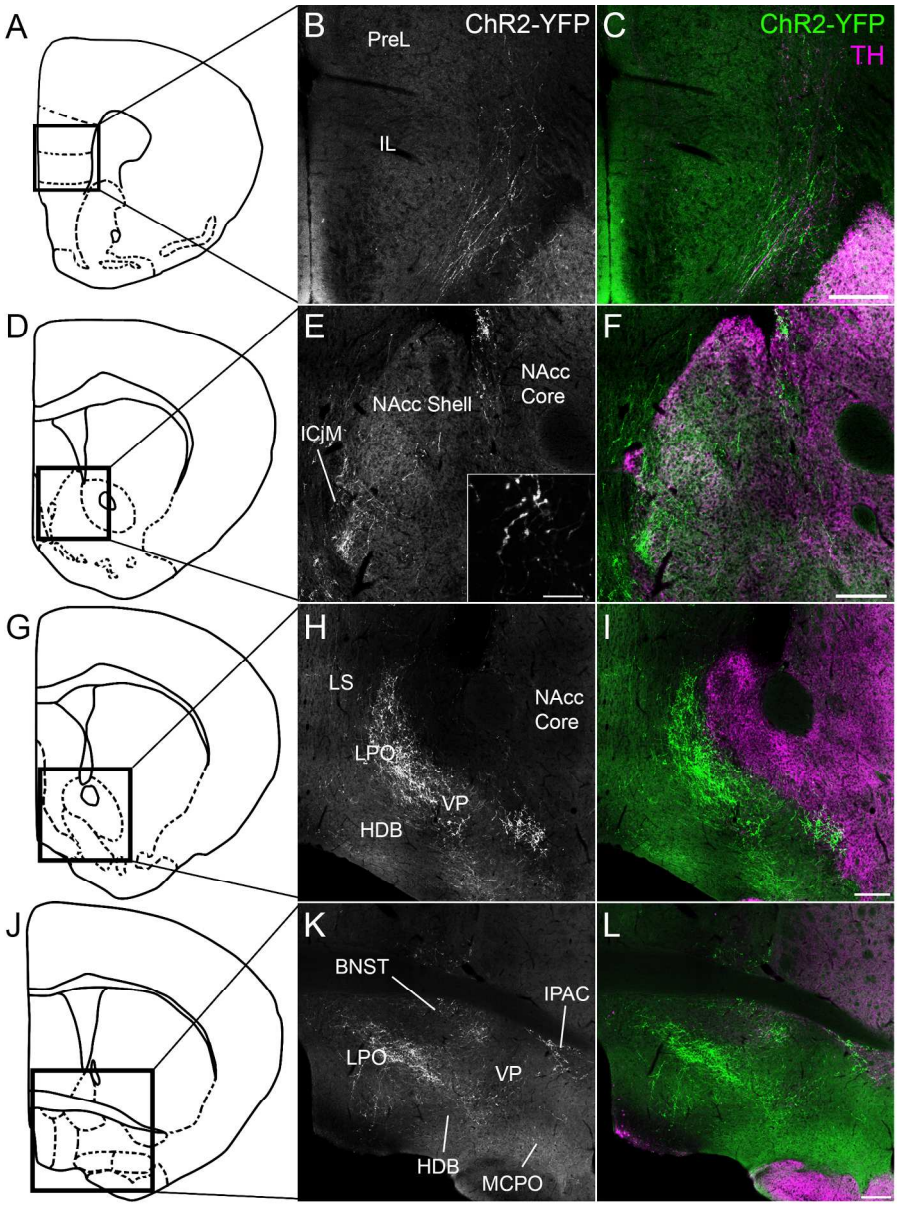

Figure 3. Panels showing anterograde labeled GABAergic fibers from case S2, which had an infusion of virus driving channelrhodopsin-eYFP, stained for eYFP (green) and TH (magenta). Panels A, D, G, and J show diagrams of forebrain sections containing labeled fibers. Black boxes indicate the regions shown in B, E, H, and K. Panels C, F, I, and L differ from B, D, F, and H only in the addition of the TH channel to delineate brain regions. Inset in Panel E shows the varicose nature of the fibers in surrounding the island of Calleja (scale bar = 10 μm). Note the largely non-overlapping patterns of GABAergic fibers and TH labeling. Scale bars in in C, F, I, L = 100 μm.
170x228mm (300 x 300 DPI)

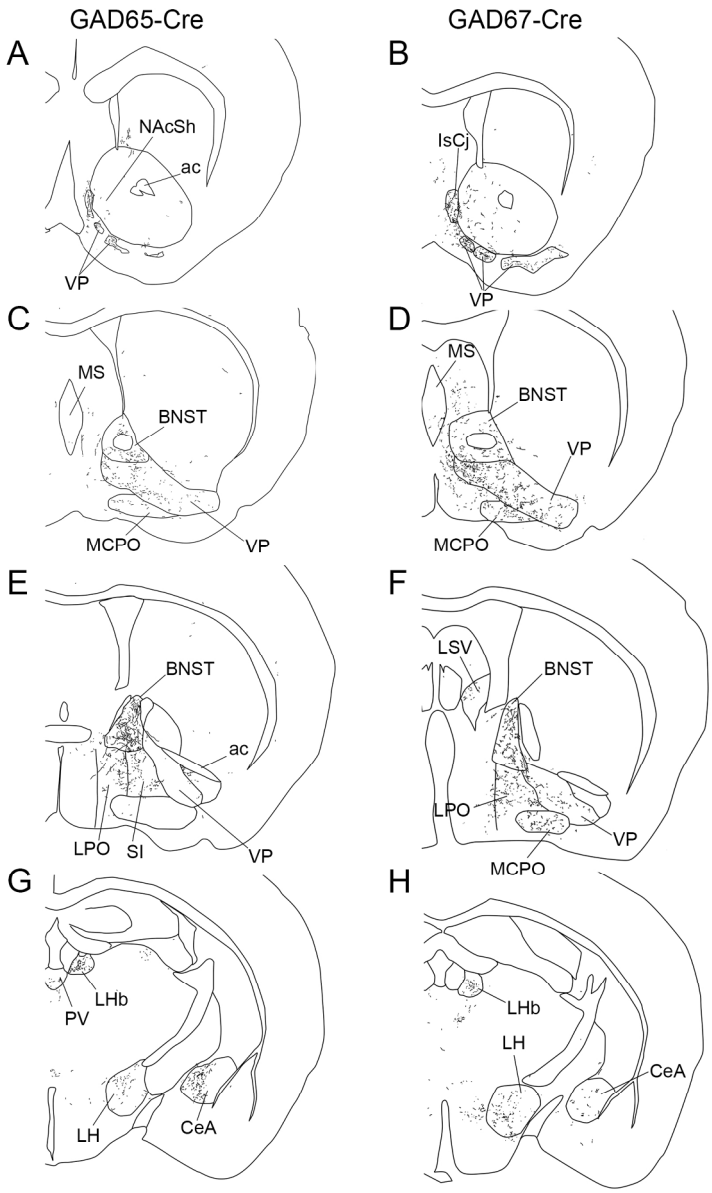

Figure 4. Coronal diagrams of line drawings of labeled fibers in representative cases from similar levels in both GAD65-IRES-Cre mice (Case S3; A, C, E, G, I, K, M, O) and GAD67-Cre mice (Case GC 153; B, D, F, H, J, L, N, P).
171x230mm (300 x 300 DPI)

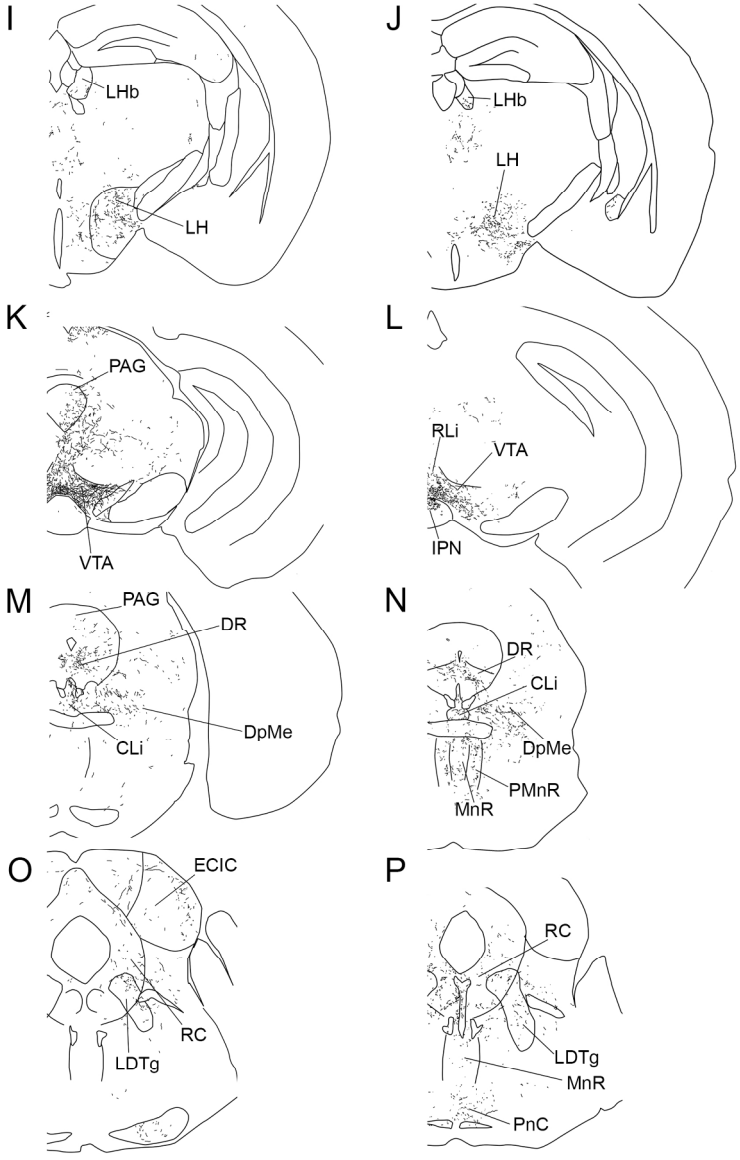

Figure 4 plate 2
171x230mm (300 x 300 DPI)

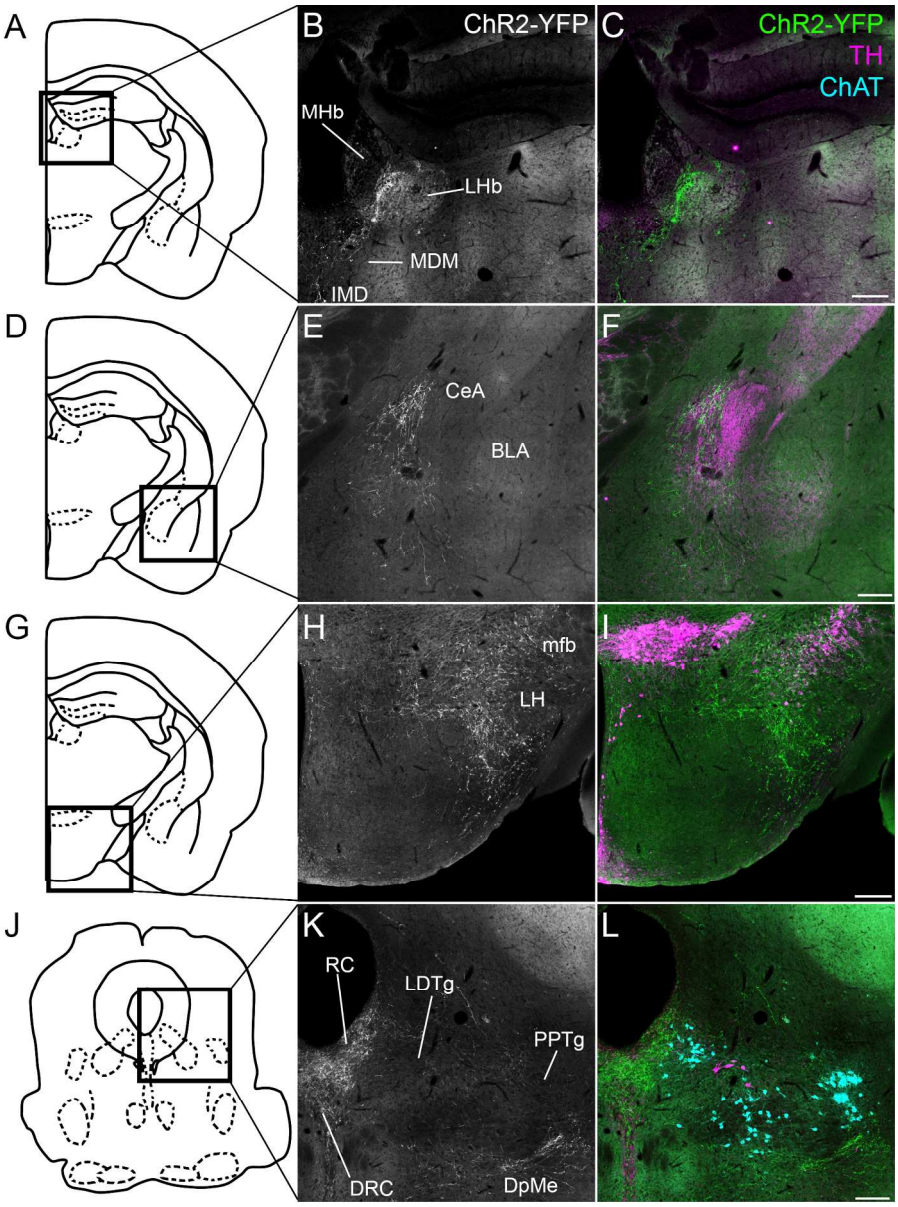

Figure 5. Panels showing images from more caudal areas of case S2 stained for channelrhodopsin-eYFP (green), TH (magenta) and ChAT (blue). Panels B, E, H, and K are enlargements of the areas outlined in A, D, G and J, respectively. Scale bars = 100 μm.
171x228mm (300 x 300 DPI)

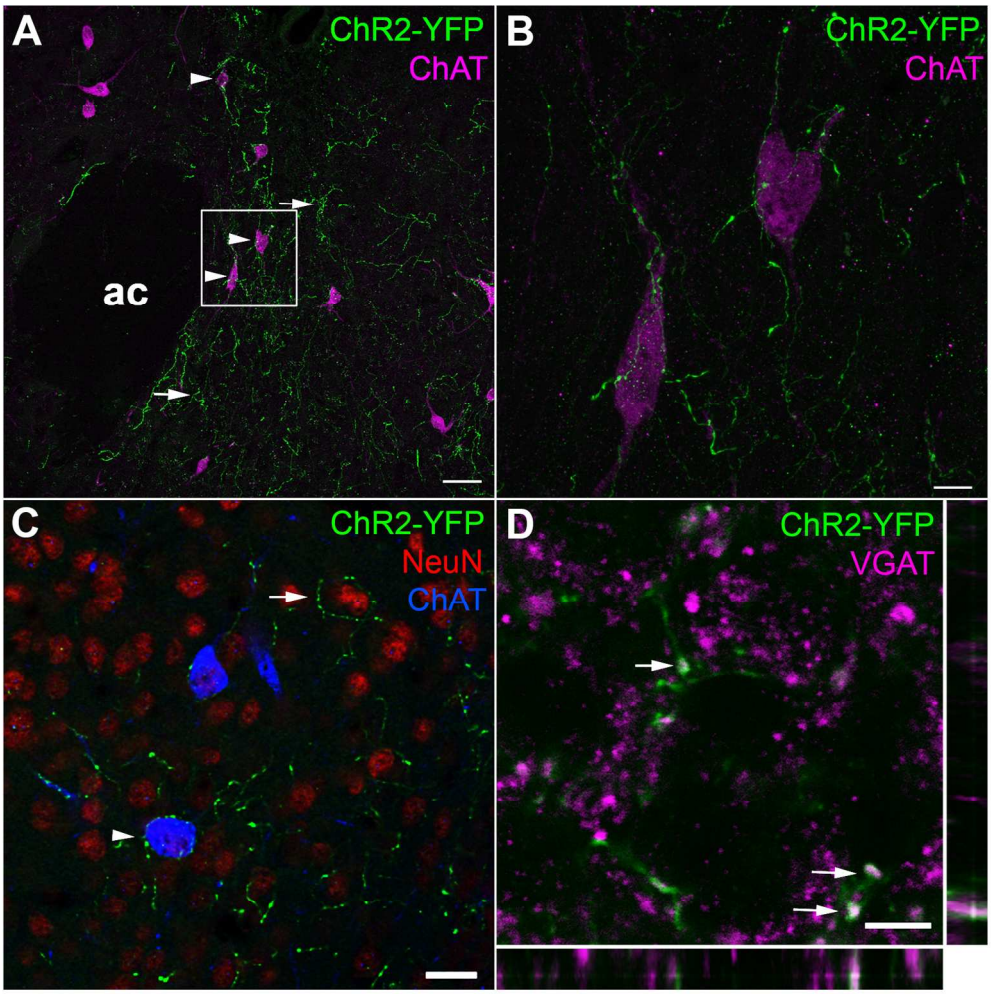

Figure 6. Ventral tegmental area GABA neurons make contact with cholinergic and non-cholinergic neurons. A) Low magnification projection image depicting GABAergic fibers apposing cholinergic cellular profiles (white arrowheads) and non-cholinergic regions (white arrows) in nucleus accumbens core (from case S2). B) High magnification projection image of outlined region in panel A. Note how the labeled fibers follow the proximal dendrites and contain several varicosities that appose the cell body and dendrites of cholinergic neurons. C) Triple labeling in nucleus accumbens shell for fibers, cholinergic cells and NeuN to reveal all neuronal nuclei suggest that GABA fibers may make similar appositions and encapsulations around non-cholinergic cells (white arrow, see white arrows in panel A). D) Co-localization of YFP+ varicosities and boutons with immunolabeling of the vesicular GABA transporter, which is localized to inhibitory synapses, indicates that these fibers are indeed GABAergic and make inhibitory connections. This image is from the lateral habenula of case S2. Similar co-labeling with VGAT is seen in LHb, CeA, VP, NAcc and VTA of both GAD67-Cre and GAD65-IRES-Cre mice. Orthogonal views are of the bouton nearest the scale bar in lower right. Scale bars in A = 50 µm; B, C = 10 µm; D = 5 µm.
154x153mm (300 x 300 DPI)

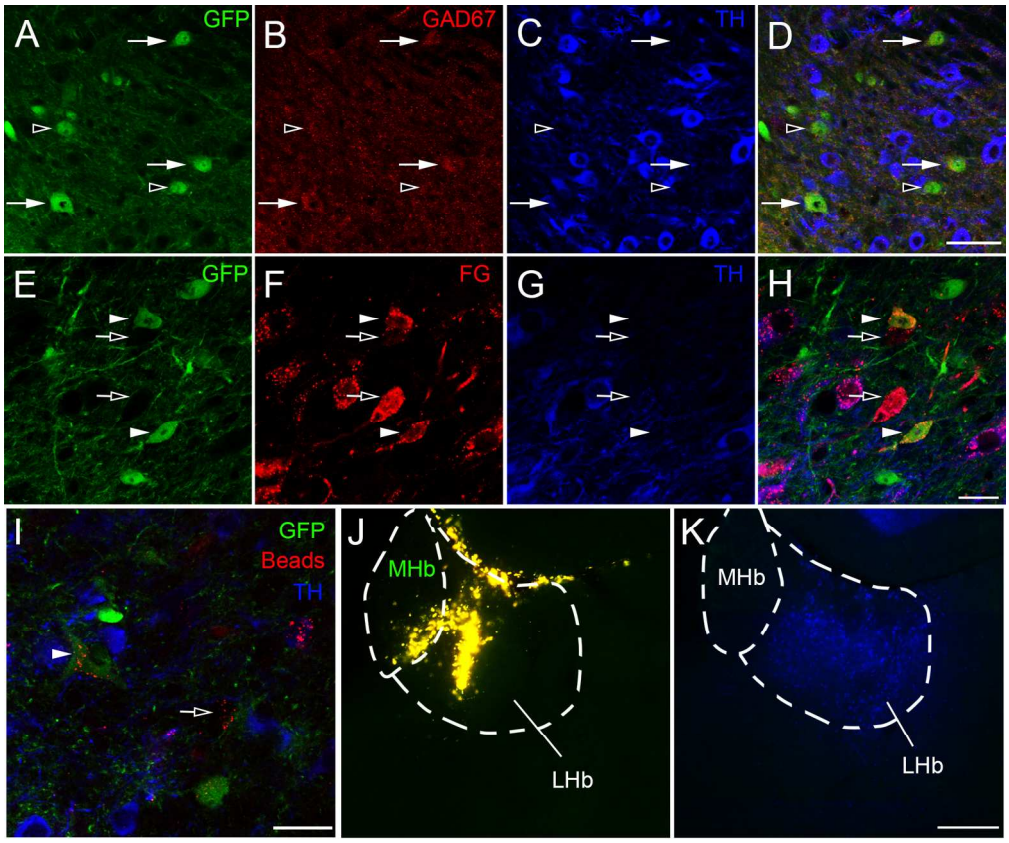

Figure 7. Retrograde tracing in GAD67-GFP knock-in mice. A-D) GFP+ cells in the VTA show immunohistochemical markers of GABA neurons (white arrows). Most, but not all GFP+ neurons (black arrowheads), clearly stain for GAD67 and lack TH immunoreactivity. Some are at the same level as surrounding neuropil. E-H) Injection of FluoroGold (FG) into the magnocellular preoptic nucleus revealed three classes of VTA projections: FG/TH (dopaminergic), FG/GFP (white arrowheads, GABAergic) and FG+ only (black arrows, TH- and GFP-; non-DA, non-GABA). I) Injections of Red Retrobeads gave similar results (white arrowhead shows a GFP+/retrogradely labeled cell, black arrow a non-TH/non-GFP/retrogradely labeled cell), here from an injection into central amygdala. J-K) Images of injections of Retrobeads (J) or FG (K) centered in lateral habenula display spread of injection. Scale bars in D = 50 μm; in H, I = 20 μm; in J, K = 100 μm.
171x143mm (300 x 300 DPI)

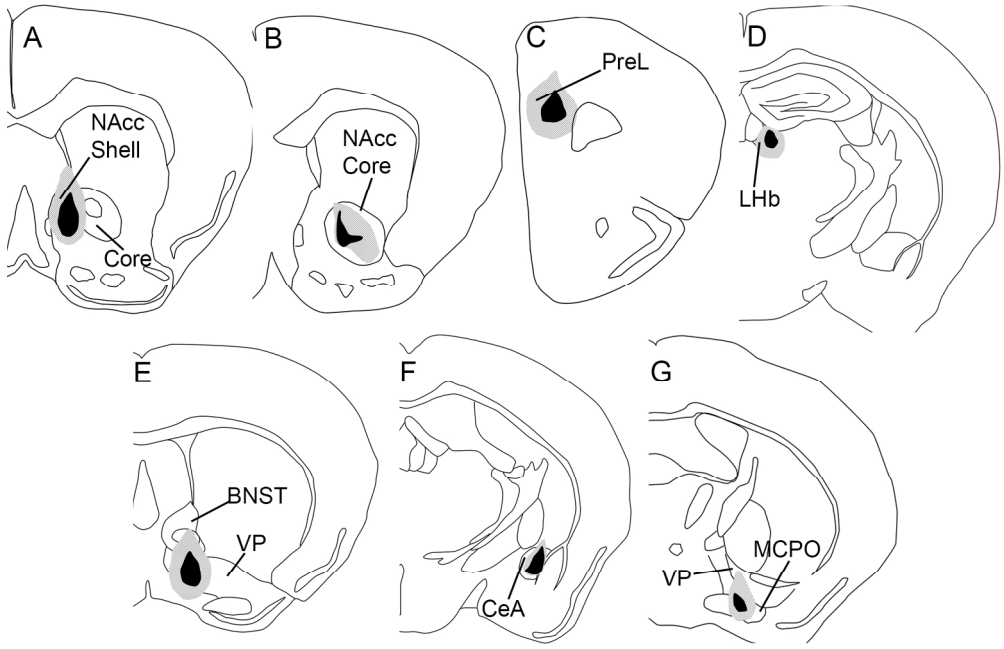

Figure 8. Diagrams of infusion sites of retrograde tracers. Tracers were infused into seven locations in GAD67-GFP knock-in mice to verify GABAergic projections. The center and spread of the tracer of a representative infusion for each target area are indicated by the filled and shaded regions, respectively. Some infusions had some minor overlap with adjacent regions.
171x115mm (300 x 300 DPI)

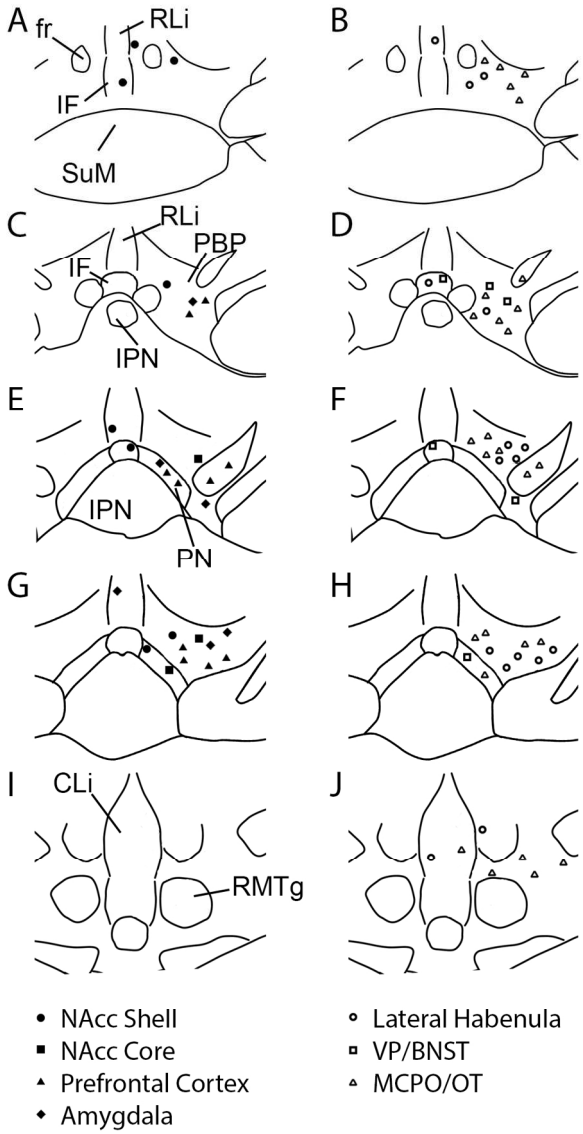

Figure 9. Coronal diagrams from rostral to caudal (A, C, E, G, I) levels of the VTA showing the location of GABA projection neurons by retrograde tracing. Panels A, C, E, G and I display cells from representative cases of infusions of tracer into NAcc Shell (filled circles), NAcc Core (filled squares), mPFC (filled triangles) and amygdala (filled diamonds). Panels B, D, F, H, and J display mark cells from cases of tracer infused into LHb (open circles), VP/BNST (open squares) and MCPO/OT (open triangles). The majority of retrogradely labeled VTA GABA neurons are found in the lateral and ventral regions of the VTA.
109x189mm (300 x 300 DPI)

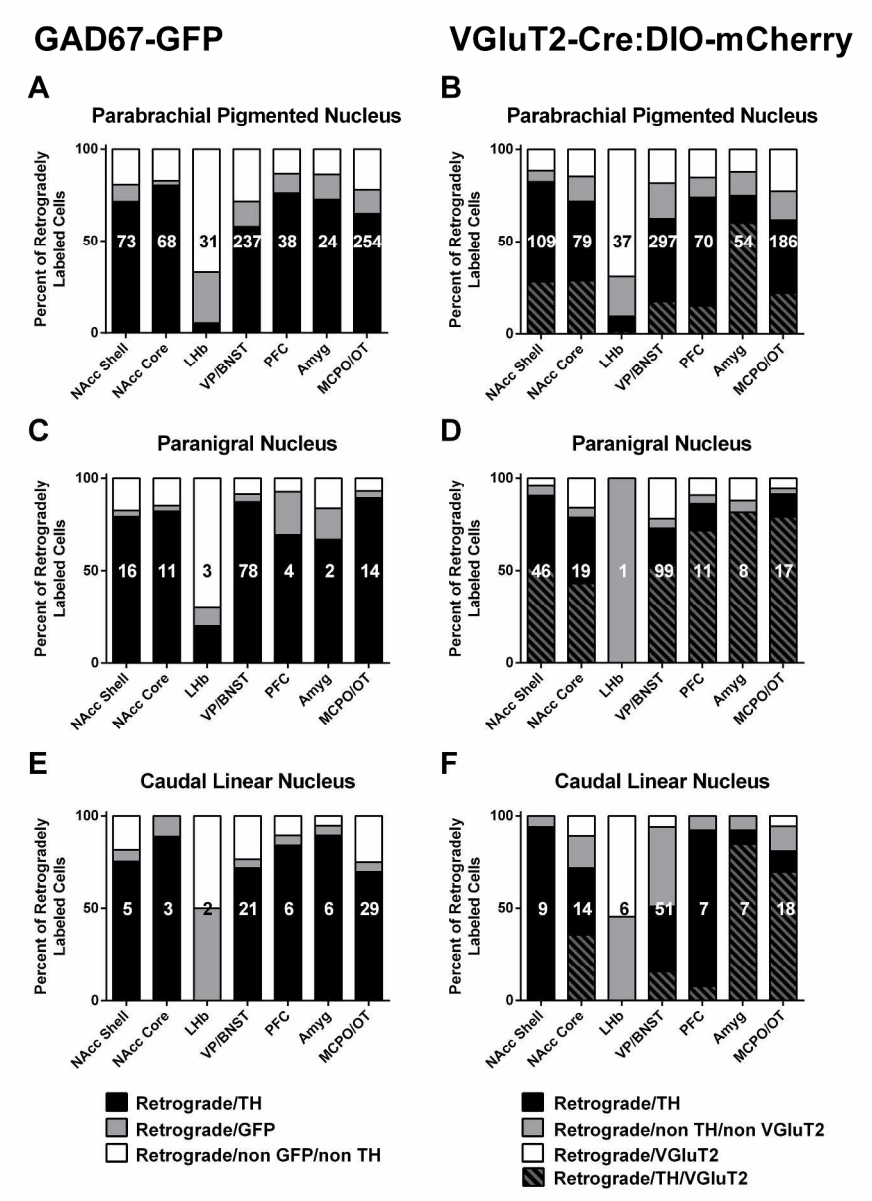

Figure 10. Graphs indicating the percentage of retrogradely labeled cells within each VTA subregion by infusion target by neurotransmitter phenotype. Panels in the left column (A, C, E, G, I) contain data from GAD67-GFP mice. Panels in the right column (B, D, F, H, J) contain data from VGluT2-IRES-Cre mice. The average number of retrogradely labeled cells per animal is contained in each column. Black indicates the percentage co-labeled for TH, black with gray stripes indicates the percentage labeled with TH and VGluT2 (VGluT2-IRES-Cre mice), gray is the percentage co-labeled for GFP (in GAD67-GFP mice) or negative for TH and VGluT2 (in VGluT2-IRES-Cre mice), and white is the percentage labeled for VGluT2 only (VGluT2-IRES-Cre mice) or negative for both TH and GFP (GAD67-GFP mice).
279x387mm (300 x 300 DPI)

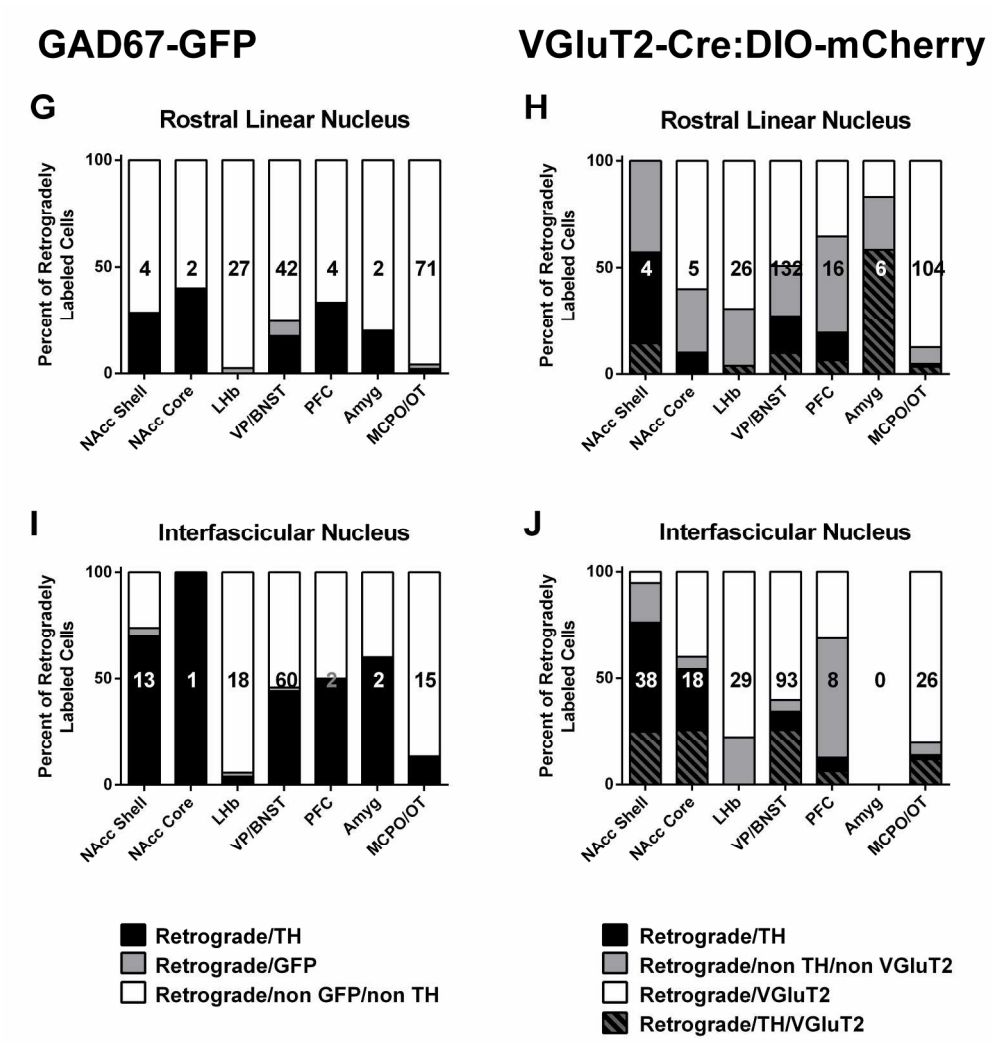

Figure 10 plate 2
211x221mm (300 x 300 DPI)

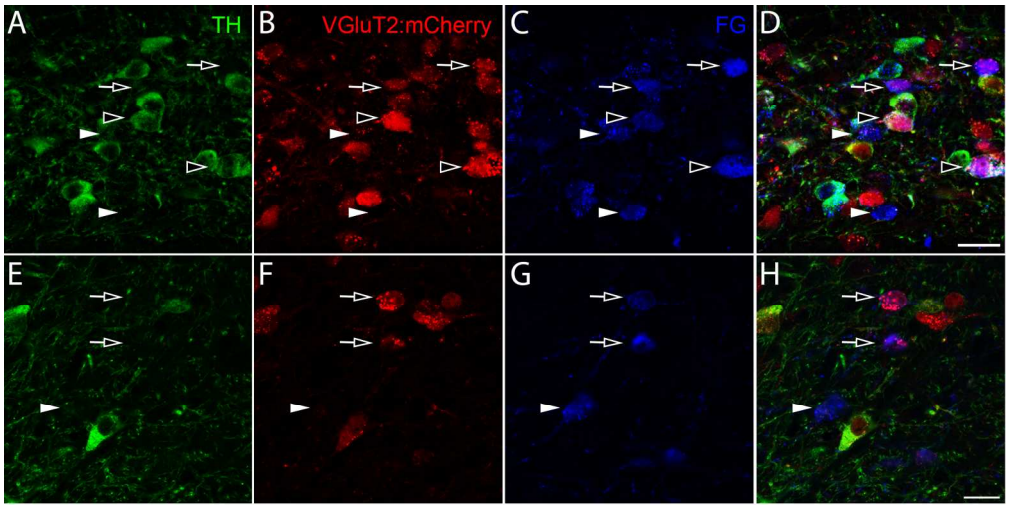

Figure 11. Retrograde tracing in VGluT2-IRES-Cre mice. Infusion of FG into MCPO (A-D) or LHb (E-H) and AAV-DIO-Ef1a-mCherry into the VTA revealed several types of projections: FG/TH only, FG/TH/VGluT2 (black arrowheads), FG/VGluT2 only (black arrows), and FG only (white arrowheads). Panels A-D show cells in the interfascicular nucleus, and panels E-H are from the parabrachial pigmented nucleus. Scale bars = 20 µm.
171x85mm (300 x 300 DPI)

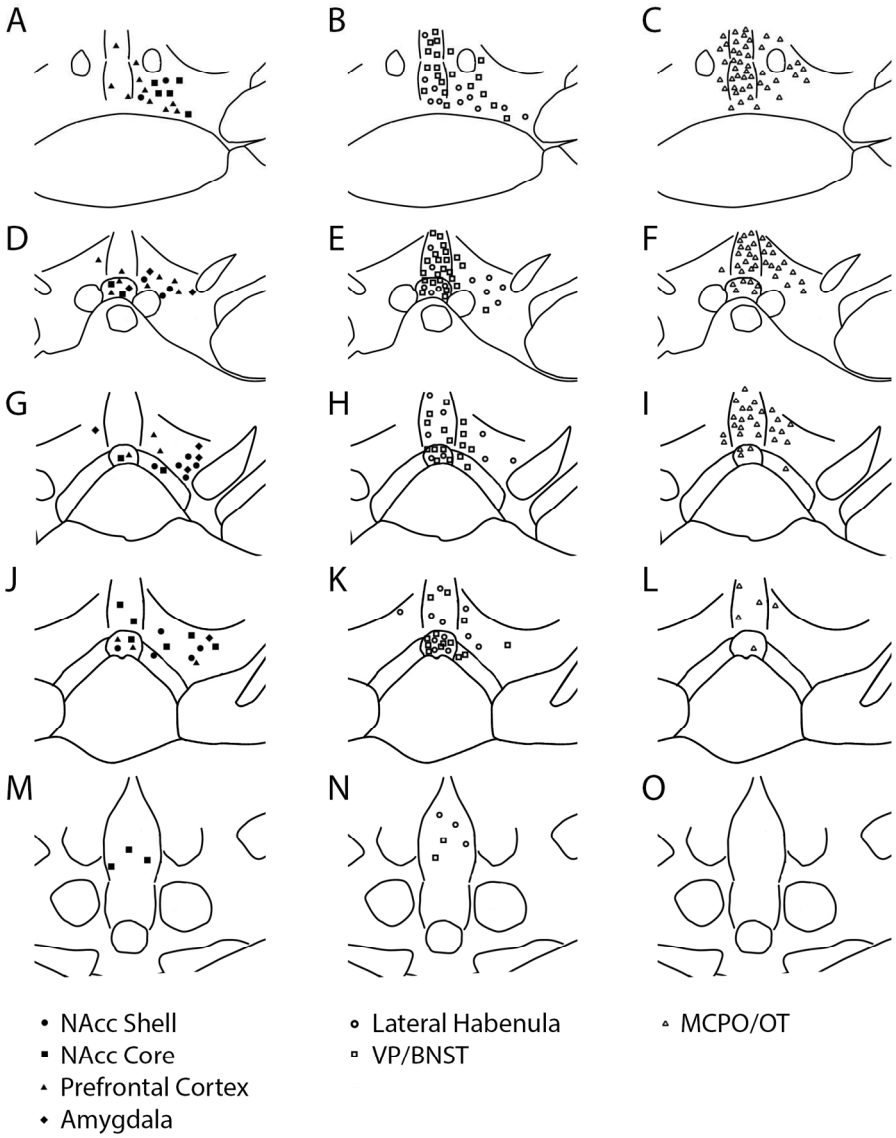

Figure 12. Coronal diagrams from rostral to caudal (top to bottom) levels of VTA showing the location of retrogradely labeled VGluT2-only neurons. One representative case from each injection site was mapped to demonstrate the location of projection neurons throughout the rostral-caudal axis of the VTA. TH+/retrogradely labeled cells were not depicted for clarity and to emphasize the non-dopaminergic projections. Note the majority of VGluT2-only projections originate from the medial nuclei (RLi and IF) and the medial portions of PBP and PN.
155x189mm (300 x 300 DPI)

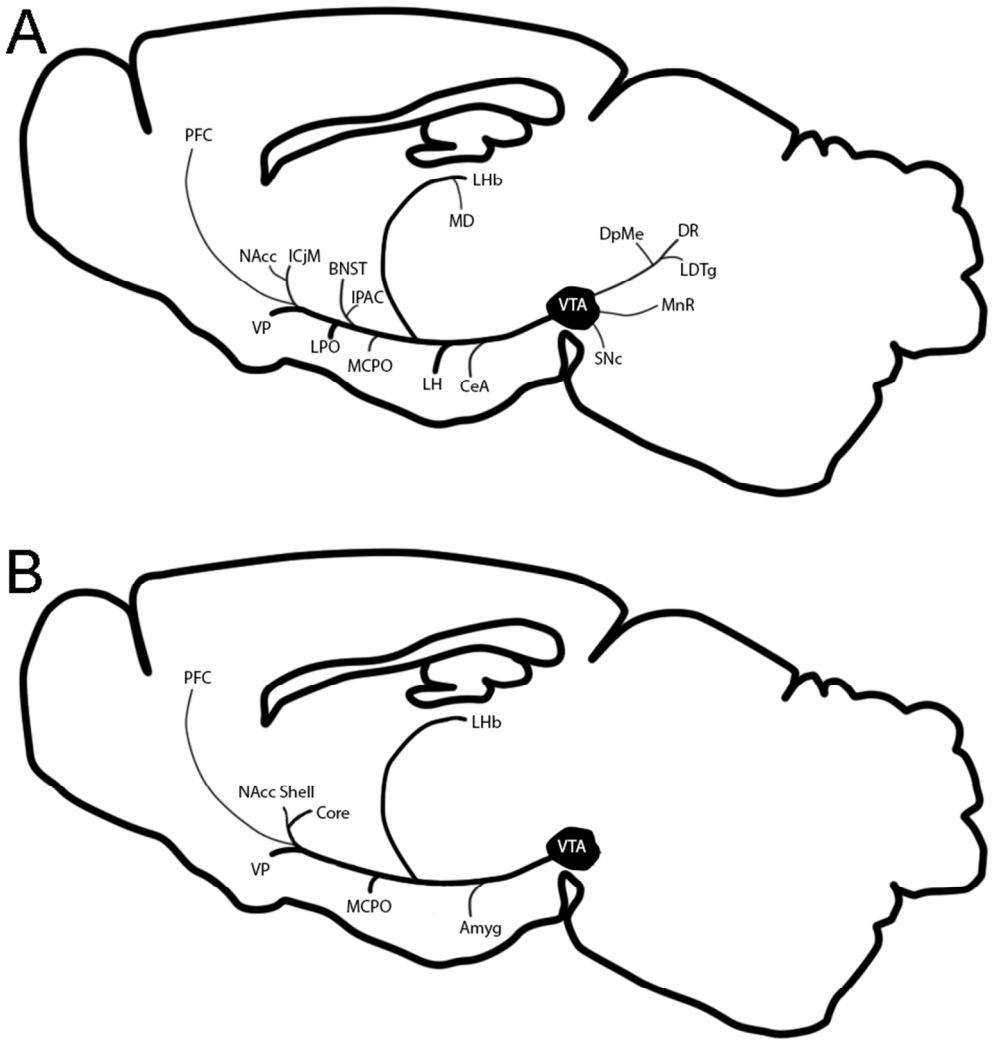

Figure 13. Summary diagram of ventral tegmental area GABAergic (Panel A) and glutamatergic (Panel B) efferents. The thickness of the arrows roughly depicts the density of the projection.
81x90mm (300 x 300 DPI)

Graphical Abstract Text

Cell-specific anterograde tracing and retrograde tracing revealed that GABAergic and glutamatergic neurons from the ventral tegmental area project to limbic structures throughout the forebrain and brainstem. The GABAergic projections were concentrated in areas that received minor dopaminergic innervation, suggesting functions for ventral midbrain GABA neurons independent of local dopamine neuron inhibition.

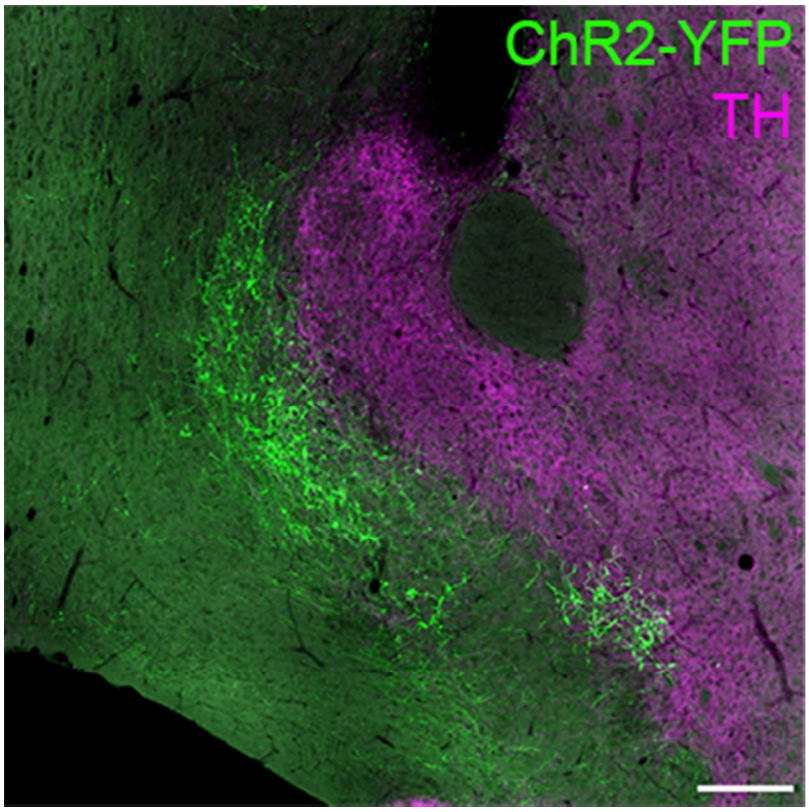

Cell-specific anterograde tracing and retrograde tracing revealed that GABAergic and glutamatergic neurons from the ventral tegmental area project to limbic structures throughout the forebrain and brainstem. The GABAergic projections were concentrated in areas that received minor dopaminergic innervation, suggesting functions for ventral midbrain GABA neurons independent of local dopamine neuron inhibition.

141x141mm (72 x 72 DPI)